

1  
2  
3  
4  
5  
6  
7  
8  
9  
10  
11  
12  
13  
14  
15  
16

## **Chapter 9**

# **Halogens in seawater, marine sediments and the altered oceanic crust and lithosphere**

Mark A. Kendrick

Research School of Earth Sciences, The Australian National University, Canberra 2601,  
Australia. [mark.kendrick@anu.edu.au](mailto:mark.kendrick@anu.edu.au)

17 **Abstract.** This chapter aims to provide a framework for understanding the distribution of  
18 halogens in the oceanic lithosphere. It reviews the concentration of F, Cl, Br and I in seawater,  
19 marine sediment pore waters, hydrothermal vent fluids, fluid inclusions from deeper in the  
20 crust, and the complementary solid-phase reservoirs of organic matter and minerals present in  
21 sediments and crustal rocks from varying depths.

22 Seawater (3.4-3.5 wt. % salt) is depleted in F, weakly enriched in I and strongly enriched in Br  
23 and Cl compared to the primitive mantle. Sequestration of I and Br by phytoplankton lead to  
24 the storage of these elements in marine sediments which are the Earth's dominant I reservoir.  
25 Regeneration of organic matter during diagenesis releases I and Br to marine sediment pore  
26 waters which can be advected into the underlying crust and lithosphere. In contrast, Cl is  
27 assumed to behave conservatively in pore waters and F is precipitated in sedimentary minerals  
28 meaning it is not significantly advected into the underlying basement.

29 Vent fluids have salinities of 0.1-6 wt. % salts, which provide evidence for phase separation  
30 and segregation of vapours and brines in hydrothermal systems. The majority of vent fluids  
31 have Br/Cl ratios within 10% of the seawater value. However, elevated Br/Cl and I/Cl ratios  
32 indicate that some vent fluids interact with sediments, and depressed Br/Cl ratios suggest some  
33 vent fluids leach Cl from glassy volcanic rocks or halite. Vent fluids have F/Cl ratios scattered  
34 around the seawater value which reflects the generally low mobility of F during diagenesis and  
35 hydrothermal alteration. In comparison to vent fluids, fluid inclusions also provide evidence  
36 for phase separation but preserve a much greater range of salinity including brines with  
37 salinities as high as ~50 wt. % salt in many parts of the crust.

38 The altered ocean crust has a F concentration of close to its initial value. In contrast, Cl is  
39 mobilised within layer 2 pillows and dykes and strongly enriched in layer 3 gabbros subjected  
40 to high temperature alteration. Amphibole is the dominant Cl host in the oceanic crust, with  
41 Cl concentrations of <500 ppm under greenschist conditions and up to wt. % levels under  
42 amphibolite conditions. The increasing Cl content of amphibole as a function of metamorphic  
43 grade most likely reflects a decreasing water/rock ratio and a general increase in fluid salinity  
44 as a function of depth in the crust. Amphibole preferentially incorporates Cl relative to Br and  
45 I; however, it is possible that I is enriched in absolute terms, and relative to Cl, in clay-rich  
46 alteration and biogenic alteration of glassy rocks in the upper crust.

47 Serpentinites formed in the oceanic lithosphere can contain thousands of ppm Cl and some  
48 serpentinites preserve Br/Cl and I/Cl signatures very similar to sedimentary pore waters,  
49 indicating that all halogens have high compatibilities in serpentine. Fluorine is slightly  
50 enriched in serpentinites compared to peridotites which may indicate mobilisation of F from  
51 igneous lithologies in the crust. Overall, the altered oceanic lithosphere reaching subduction  
52 zones is estimated to have a maximum median Cl content of ~400 ppm, and it is estimated to  
53 have a F/Cl ratio of ~0.25 compared to ~2 in pristine crust. It is therefore estimated that  
54 approximately 90% of the Cl present in altered oceanic lithosphere is introduced during  
55 seawater alteration.

56

## 57 **9.1 Introduction**

58           As a chemical group, the halogens (F, Cl, Br, I) are united by the ability to form  
59 negatively charged anions; however, Cl is uniquely important within this group because it is  
60 the dominant ligand that enables metal transport in the majority of hydrothermal solutions  
61 (Bischoff and Dickson, 1975; Seyfried and Bischoff, 1981; Yardley, 2005). Fluid salinity is  
62 consequently of profound importance to the mass transfer processes operating during  
63 hydrothermal alteration of the oceanic lithosphere. There is wide interest in the scale of  
64 seafloor alteration processes and metasomatism because alteration of the oceanic lithosphere  
65 moderates the composition of seawater (Bischoff and Dickson, 1975; Edmond et al., 1979) and  
66 determines the chemical composition of the slab that is subducted into the mantle at convergent  
67 plate margins meaning that seafloor alteration is critical to the geological cycles of all elements  
68 (Spandler and Pirard, 2013).

69           In comparison to Cl, the other halogens exhibit systematically different behaviours in  
70 the oceanic lithosphere that are related to their ionic sizes or elemental abundances. Fluorine  
71 and Cl are similarly abundant on Earth with primitive mantle concentrations on the order of  
72 ~15-25 ppm (Table 1; Pyle and Mather, 2009). However, the F<sup>-</sup> anion is significantly smaller  
73 than the heavier halogens and F is strongly electronegative, being the only element in the  
74 periodic table that is more electronegative than oxygen. These properties result in F having a  
75 much higher compatibility than Cl in many hydrous and nominally anhydrous minerals  
76 (Bernini et al., 2013; Carpenter, 1969; Dalou et al., 2012; Frohlich et al., 1983; Ichikuni, 1979;  
77 Seyfried and Ding, 1995). In addition, F is distinguished from the heavier halogens by a low  
78 solubility in aqueous fluids (Seyfried and Ding, 1995).

79           Bromine and I have even higher solubilities in aqueous fluids than Cl, but they are trace  
80 constituents on Earth with primitive mantle concentrations of less than ~60 ppb for Br and less  
81 than ~10 ppb for I (Table 1). Iodine is a weakly electronegative redox sensitive element that

82 is important in a number of biochemical pathways, which together with its low abundance  
83 mean it is regarded as an essential element for life (Elderfield and Truesdale, 1980; Fuge and  
84 Johnson, 1986; Leblanc et al., 2006).

85         The contrasting solubilities of F, Cl, Br and I in aqueous fluids mean that their relative  
86 abundances, or the F/Cl, Br/Cl and I/Cl, ratios of a fluid, can provide useful information about  
87 a number of hydrogeochemical processes relevant to alteration of the oceanic lithosphere.  
88 These include the roles of phase separation, crustal-hydration, dissolution of evaporites, or  
89 precipitation of hydrothermal-halite in controlling vent fluid salinity (Campbell and Edmond,  
90 1989; Oosting and Von Damm, 1996; Seyfried et al., 2003; You et al., 1994). In addition, the  
91 presence of organic matter can be inferred from high I abundances (Campbell and Edmond,  
92 1989; Gieskes et al., 2002; Kawagucci et al., 2011). This information is of considerable  
93 importance to investigating the role of fluids in alteration of the oceanic lithosphere and the  
94 depth of the biosphere (Campbell and Edmond, 1989; Mottl et al., 2011; Oosting and Von  
95 Damm, 1996; Reeves et al., 2011; Wu et al., 2012; You et al., 1994).

96         The current chapter aims to show how the different geochemical behaviours of the  
97 halogens control their abundances in both hydrothermal fluids and the complementary  
98 reservoirs of the oceanic lithosphere and how salts, and acids generated by hydrolysis of salts,  
99 facilitate transport of metals in solution (Seyfried and Bischoff, 1981). The majority of data  
100 for both altered oceanic rocks and fluids are for Cl, with more limited data available for F and  
101 Br, and very limited data for I. Therefore while the aim is to provide a framework for  
102 understanding the distribution of halogens in the oceanic lithosphere, an important role of this  
103 chapter is also to identify current gaps in our knowledge. Improving constraints on the absolute  
104 and relative abundances of F, Cl, Br, and I in different lithospheric reservoirs (e.g. sediments,  
105 altered basalt, serpentinites) is critical for optimal use of halogen abundance ratios in tracking  
106 halogens through the subduction cycle (Kendrick et al., 2012b; Straub and Layne, 2003) and

107 will further contribute to our understanding of marine halogen cycling (Frohlich et al., 1983;  
108 Leblanc et al., 2006; Seyfried et al., 1986; Seyfried and Ding, 1995).

109

## 110 **9.2 Halogen chemistry in seawater and marine sediments**

111 The halogen composition of seawater and the more evolved fluids that have interacted with  
112 sediments and could be advected into the mafic portions of the oceanic lithosphere is controlled  
113 by the unique chemical properties of each halogen and their abundances on Earth.

114 The concentrations of F, Cl and Br in seawater, present as the fluoride ( $F^-$ ), chloride  
115 ( $Cl^-$ ), and bromide ( $Br^-$ ) anions, is fairly constant over thousand-year timescales with minor  
116 variations related to salinity which fluctuates around ~3.4-3.5 wt. % salts (Drever, 1997; Pinet,  
117 1992). In contrast, I is unique among the halogens because its predominant species in seawater  
118 is iodate ( $IO_3^-$ ) and iodide ( $I^-$ ) is only important in surface waters and small anoxic basins  
119 (Elderfield and Truesdale, 1980; Huang et al., 2005; Wong and Brewer, 1977). The  
120 concentration of iodate, which is taken up by a number of marine organisms, is correlated with  
121 other nutrients such as nitrate and phosphate and varies as a function of water depth and latitude  
122 (Elderfield and Truesdale, 1980; Huang et al., 2005). In addition to iodate and iodide, dissolved  
123 organic I is significant at shallow and intermediate depths accounting for up to ~5 ppb of the  
124 total I at depths of 400 m in the north Pacific (Huang et al., 2005). The total I concentration of  
125 seawater varies from about 44 ppb up to 76 ppb with a mean of ~58 ppb (Elderfield and  
126 Truesdale, 1980; Huang et al., 2005; Nakayama et al., 1989; Zheng et al., 2012).

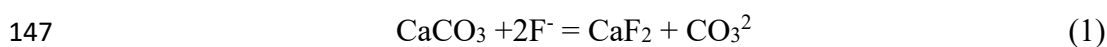
127 The average abundances of halogens in seawater (Drever, 1997; Elderfield and  
128 Truesdale, 1980; Huang et al., 2005) and estimated abundances of halogens in the primitive  
129 mantle (McDonough and Sun, 1995; Palme and O'Neill, 2003; Sharp and Draper, 2013) are  
130 given in Table 1. Recent estimates for primitive mantle Cl, Br and I still vary by a factor of

131 ten (e.g. Pyle and Mather, 2009); however, the representative values in Table 1 illustrate that  
132 F is unique among the halogens because it is depleted in seawater relative to the primitive  
133 mantle (Table 1). In comparison, I exhibits a modest enrichment in seawater and Cl and Br are  
134 both enriched by ~1000 times in seawater compared to the primitive mantle (Table 1).

135

### 136 *9.2.1 Fluorine's low solubility*

137 The low solubility of F in aqueous fluids means that in contrast to the heavy halogens  
138 (Cl, Br and I), F is inefficiently transported by rivers, and is removed from solution once in the  
139 ocean (Carpenter, 1969). Important F sinks in the oceanic environment include marine  
140 carbonates, phosphates, and alumina-silicate clay minerals (cf. Carpenter, 1969; Frohlich et al.,  
141 1983; Matthies and Troll, 1990; Rude and Aller, 1994). Calcite can contain hundreds of ppm  
142 of F (Fig 1). Magnesium-calcite and aragonite have maximum F concentrations in excess of  
143 1000 ppm that represent a 1000-fold enrichment over seawater and demonstrate the high  
144 compatibility of F in carbonate (Fig 1; Ohde and Kitano, 1980; Okumura et al., 1983; Opdyke  
145 et al., 1993; Rude and Aller, 1991; Tanaka et al., 2013). An exchange reaction has been  
146 proposed in which two F<sup>-</sup> anions substitute for CO<sub>3</sub><sup>2-</sup> (Ichikuni, 1979):



148 Given the conservative nature of F<sup>-</sup> in seawater, the implication of this reaction is that the F  
149 content of aragonite can be used to monitor the CO<sub>2</sub> content of seawater, which exhibits  
150 significant spatial and temporal variation (e.g. Ichikuni, 1979; Ramos et al., 2005; Tanaka et  
151 al., 2013).

152 Carbonate fluorapatite (CFA) in marine phosphates with concentrations of 1-3 wt. % F  
153 contains an order of magnitude more F than carbonate (Li and Schoonmaker, 2003; Rude and

154 Aller, 1991). However, because phosphorite deposits are restricted to zones of nutrient rich  
155 water upwelling they are estimated to account for only ~20% of F uptake from the ocean  
156 (Frohlich et al., 1983). Fluorine also substitutes for the hydroxyl group in alumina-silicate  
157 clay minerals; however, the relative importance of this sink is disputed (cf. Carpenter, 1969;  
158 Matthies and Troll, 1990; Rude and Aller, 1994).

159 Fluorine is mobilised during diagenesis of marine carbonates but it is fixed into newly  
160 formed carbonates, apatite, or clay minerals, meaning the fluids occupying sediment pore  
161 spaces have low ppm levels of F and F/Cl ratios similar to seawater (Frohlich et al., 1983;  
162 Mahn and Gieskes, 2001; Rude and Aller, 1994).

163 Fluorine is further distinguished from the heavier halogens by its relative compatibility  
164 in the mantle. Fluorine has a compatibility comparable to moderately incompatible elements  
165 like Nd (Workman et al., 2006), whereas the heavy halogens (Cl, Br and I) have  
166 incompatibilities comparable to more strongly incompatible elements such as K, La or Nb  
167 (Kendrick et al., 2012a; le Roux et al., 2006; Schilling et al., 1980). This difference cannot  
168 explain the F depletion of seawater but it does imply the surface reservoirs of seawater and  
169 sediments are less enriched in F than the heavy halogens (cf. Table 1).

170

### 171 ***9.2.2 Chlorine in halite***

172 In contrast to F, Cl is often regarded as a conservative element in sedimentary marine pore  
173 waters, meaning its concentration is not easily altered. Chlorine and Br have very low  
174 compatibilities in marine carbonate (Kitano et al., 1975; Okumura et al., 1986) and low  
175 concentrations in other sedimentary minerals such as carbonate fluorapatite. As a result,  
176 evaporites formed by evaporation of seawater beyond the point of halite saturation (30-35 wt.

177 % salt; McCaffrey et al., 1987; Zherebtsova and Volkova, 1966), commonly represent the only  
178 significant mineral reservoir of Cl in sedimentary settings (Hanor, 1994; Worden, 1996).  
179 Evaporite deposits are important sedimentary units in some ocean basins and dissolution of  
180 evaporites is indicated as an important source of salinity for hydrothermal fluids in Red Sea  
181 brine pools (e.g. Pierret et al., 2001; Shanks and Bischoff, 1977; Zierenberg and Shanks III,  
182 1986). In addition, halite could be important in some hydrothermal settings where precipitation  
183 of hydrothermal halite is possible (Butterfield et al., 1997; Foustoukos and Seyfried, 2007).

184         Evaporitic salt deposits are characterised by very low Br/Cl and I/Cl ratios (Bein et al.,  
185 1991; Fontes and Matray, 1993; McCaffrey et al., 1987). Halite has partition coefficients ( $D$   
186 =  $R_{\text{salt}}/R_{\text{fluid}}$ ) of  $\sim 0.03$  for Br/Cl and  $< 0.003$  for I/Cl, whereas Br can be accommodated more  
187 easily in sylvite ( $D \sim 0.2$ ), carnalite, and other potash salts (Fontes and Matray, 1993; Hermann,  
188 1980; Holser, 1979; Siemann and Schramm, 2000). As a result, the actual concentrations of  
189 Br and I in evaporite deposits vary depending on the salts present; on the presence of organic  
190 material and fluid inclusions which contain significant Br and I; and on the diagenetic history  
191 of the deposit (Bein et al., 1991; Fontes and Matray, 1993). Experimental studies suggest Br  
192 is excluded from the halite lattice under hydrothermal conditions (Berndt and Seyfried, 1997;  
193 Foustoukos and Seyfried, 2007). This means that fluid interaction with either sedimentary or  
194 hydrothermal halite has the potential to strongly alter Cl concentrations and fluid Br/Cl and  
195 I/Cl ratios.

196

### 197 ***9.2.3 Iodine and bromine in organic matter***

198 The marine I cycle is dominated by accumulation of I in algae: Kelp (a type of seaweed, which  
199 is multicellular macroalgae) is the main I accumulator in coastal environments, whereas



200 phytoplankton is the main I accumulator at sea (Iwamoto and Shiraiwa, 2012; Leblanc et al.,  
201 2006).

202 Iodine is seasonally variable and heterogeneously distributed in Kelp (Gall et al., 2004).  
203 Maximum concentrations of ~6 wt.% I have been reported in parts of a Kelp plant (*Laminaria*  
204 *Digitalis*; Kuepper et al., 2013), but an average I content of 1 wt. % has been suggested (Gall  
205 et al., 2004). Other seaweeds contain ~1-500 ppm I (Muramatsu and Wedepohl, 1998; Yang  
206 et al., 2014). Several species of coral have skeletons in which organic components can have  
207 very high halogen concentrations of 5-6 wt. % I, 1-2 wt. % Br, and <1000 ppm Cl (Collins,  
208 1969; Goldberg et al., 1994). The Br/I weight ratios of seaweeds and corals range from ~0.1  
209 to 2.5 (Collins, 1969; Kuepper et al., 2013). In comparison, plankton has variable halogen  
210 contents ranging from sub-ppm to typical values of ~200 to 300 ppm I and 1000 to 4000 ppm  
211 Br. Plankton have Br/I weight ratios of 3-24 and I/C<sub>organic</sub> of 0.0002-0.002 (Bobrov et al., 2005;  
212 Iwamoto and Shiraiwa, 2012; Martin et al., 1993; Price and Calvert, 1977).

213 Iodine accumulated by algae is either emitted to the atmosphere as I<sub>2</sub> gas (or volatile  
214 iodocarbon compounds) or buried in marine sediment, which has previously been estimated to  
215 contain ~70% of the I present in the crust and seawater (Leblanc et al., 2006; Muramatsu and  
216 Wedepohl, 1998). Regeneration of organic matter releases iodide (I<sup>-</sup>), bromide (Br<sup>-</sup>), and CH<sub>4</sub>  
217 into sedimentary pore waters in the subsurface (Kennedy and Elderfield, 1987a, b; Muramatsu  
218 et al., 2007; Price and Calvert, 1973, 1977). Studies of cosmogenic <sup>129</sup>I indicate pore waters  
219 can migrate laterally over many km (e.g. Fehn et al., 2006; Muramatsu et al., 2001; 2007).  
220 However on average, pore waters seep gradually upwards toward the seafloor (Wong and  
221 Brewer, 1977). In typical oxic basins, iodide in escaping pore waters is oxidised and, together  
222 with seawater iodate, is then adsorbed back onto organic detritus close to the sediment surface  
223 (Fig 2; Price and Calvert, 1973, 1977). If present, additional adsorption may also occur on Fe-  
224 hydroxides (Ullman and Aller, 1985) and clay minerals (Montavon et al., 2014). As a result

225 sediment profiles in oxic basins can have very high I concentrations of 100-2000 ppm close to  
226 the surface (Fig 2a; Price and Calvert, 1977), along with elevated  $I/C_{\text{organic}}$  and  $I/\text{Br}$  ratios, but  
227 at depths of more than a metre below the surface sediments have more typical concentrations  
228 of ~5-50 ppm I, along with  $I/C_{\text{organic}}$  and  $I/\text{Br}$  ratios similar to plankton (Kennedy and  
229 Elderfield, 1987a, b; Price and Calvert, 1973, 1977; Upstillgoddard and Elderfield, 1988).

230 Halogen regeneration processes result in pore water Br and I concentrations which tend  
231 to increase with depth and solid phase Br and I concentrations which tend to decrease with  
232 depth and sediment maturity (Fig. 2). Pelagic sediments have typical I concentrations of ~5-  
233 50 ppm I in the solid phase (Kennedy and Elderfield, 1987b; Muramatsu et al., 2007).  
234 However, Muramatsu et al (2007) reported that sediments from the Nankai Trough contain 3-  
235 4 times more Br and I in pore waters than in the solid phase. In contrast to unconsolidated  
236 sediment, lithified marine sediments have much lower halogen concentrations. For example,  
237 the median I concentration of twenty limestones and shales analysed by Muramatsu and  
238 Wedepohl (1998) is  $2^{+2}_{-1}$  ppm. The Callovian-Oxfordian clay of France contains 1 to 7 ppm I  
239 and 0.4 to 1.2 wt. % organic C (Claret et al., 2010). The organic rich Kimmeridge clay of  
240 England contains 6 to 34 ppm I and 16 to 55 wt. % organic C (Cosgrove, 1970). Taken together,  
241 these data give a combined average of  $4 \pm 3$  ppm I in lithified marine sediments (Table 2) and  
242 suggest that variable depletion of I occurs relative to C in lithified sediments, compared with  
243 organic I/C ratios.

244 A large database is now available for Cl, Br and I in sedimentary marine pore waters  
245 (Fig 3; Fehn et al., 2000; 2003; 2006; 2007ab; Gieskes and Mahn, 2007; Mahn and Gieskes,  
246 2001; Martin et al., 1993; Muramatsu et al., 2001; 2007; Tomaru et al., 2007abc; 2009). These  
247 studies have shown that sedimentary pore waters have a relatively narrow range in salinity (~1-  
248 5 wt. % salt), which reflects the modification of seawater salinity (3.5 wt. % salts) by formation  
249 and destruction of gas hydrate (Fig 3b). Plotting pore fluid Cl, Br, and I data as ratios in a three

250 element plot, which removes the effects of salinity variation, enables the sediment-derived  
251 halogen component to be fully resolved from seawater (Fig 3a). The slopes in Fig 3a indicate  
252 that the sediment-derived halogen component has a fairly constant seawater-corrected Br/I  
253 weight ratio of ~0.3-1.6 (Fig 3a; Kendrick et al., 2011a). The low seawater-corrected Br/I ratio  
254 of sedimentary pore waters (0.3-1.6), compared to plankton (3-24; Bobrov et al., 2005; Collins,  
255 1969; Martin et al., 1993), reflects preferential mobilisation of I compared to Br during  
256 diagenesis, with the excess I representing the surface-adsorbed I component acquired under  
257 oxic conditions (Francois, 1987; Martin et al., 1993; Upstillgoddard and Elderfield, 1988). In  
258 comparison, the solid sedimentary phase preserves higher Br/I ratios, which are similar to  
259 planktonic values (Fig 3; Muramatsu et al., 2007).

260

#### 261 ***9.2.4 Iodine adsorption and substitution in carbonate***

262 In addition to I sorption onto organic detritus at the sediment-seawater interface (Price and  
263 Calvert, 1973, 1977), I is significantly adsorbed onto the surfaces of a number of reactive  
264 minerals (Ullman and Aller, 1985). Available data indicate that hydrogenetic Fe-Mn crusts  
265 formed on igneous substrates, and nodules formed in sedimentary environments, contain up to  
266 390 ppm F, 1.1 wt. % Cl, 200 ppm Br and 900 ppm I which represent a factor of ~2 depletion  
267 of Cl, a factor of ~3 enrichment of Br, a factor of ~300 enrichment of F and a factor of ~2000  
268 enrichment of I compared to seawater (Table 2; Glasby, 1973; Glasby et al., 1978; Hein and  
269 Koschinsky, 2014; Rude and Aller, 1991). Hydrogenetic Fe-Mn crusts and nodules include  
270 detrital minerals such as fluorapatite and a mixture of MnO<sub>2</sub> and FeOOH precipitated from  
271 cold seawater (with a varying hydrothermal component in some cases; Baturin and Dubinchuk,  
272 2011; Hein and Koschinsky, 2014). The crusts have slow growth rates, very high porosities,  
273 and large reactive surface areas that enable efficient scavenging of reactive trace elements from

274 seawater (Hein and Koschinsky, 2014). The experiments of Ullman and Aller (1985) confirm  
275 iodate, but not iodide, is strongly adsorbed onto Fe-oxyhydroxides and the same may be true  
276 for Mn oxide crusts.

277 Clay minerals such as montmorillonite  $[(\text{Na,Ca})_{0.33}(\text{Al,Mg})_2(\text{Si}_4\text{O}_{10})(\text{OH})_2.n\text{H}_2\text{O}]$  have  
278 reactive surfaces that adsorb variable quantities of water (e.g.  $n\text{H}_2\text{O}$ ) and other substances. Due  
279 to the environmental significance of radioactive iodide, which is one of the most mobile  
280 radioisotopes present in nuclear waste, a number of investigations have been conducted to  
281 evaluate the sorption of I to clay. Experimental results showing significant I sorption have been  
282 controversial because of uncertainties regarding the speciation of I in the experiments (Glaus  
283 et al., 2008), and the potential of I to be irreversibly bound in carbonate formed during the  
284 experiment (Claret et al., 2010). However, a recent study that controlled for these factors  
285 reported reversible sorption of iodide onto clay minerals under controlled  $\text{PCO}_2$  (Montavon et  
286 al., 2014).

287 Claret et al. (2010) suggested carbonate within Callovian-Oxfordian clay rock (France)  
288 contains  $\sim 2$  ppm I. Recent experimental data suggest that  $\text{IO}_3^-$  but not  $\text{I}^-$  can substitute for  $\text{CO}_3^{2-}$   
289 in calcite (Lu et al., 2010) and the iodate mineral lautarite  $[\text{Ca}(\text{IO}_3)_2]$  is known from I-rich  
290 nitrate deposits (Jackson and Ericksen, 1997). In contrast,  $2\text{F}^-$  can readily substitute for  $\text{CO}_3^{2-}$   
291 , but  $\text{Br}^-$  and  $\text{Cl}^-$  (like  $\text{I}^-$ ) have low compatibilities in carbonate (Kitano et al., 1975; Okumura  
292 et al., 1986). It should however, be noted that while the maximum I concentration of 2 ppm  
293 reported for carbonate represents a considerable enrichment over seawater I concentration of  
294  $\sim 58$  ppb, it is 100 times less than the maximum I concentration of  $\sim 220$  ppm in sedimentary  
295 pore waters (Table 2). Further work is clearly required to understand the interactions of I  
296 species, clay minerals and carbonates.

297

298 **9.2.5 Summary**

299 Two distinct fluids that could be advected into the mafic portions of the oceanic crust have  
300 been identified and are relatively well defined: i) seawater and ii) sedimentary marine pore  
301 water. Sedimentary marine pore waters comprise seawater modified by the addition of organic  
302 components and adsorbed I present in marine sediments. The majority of pore waters preserve  
303 salinities close to seawater, but salinities of 1-5 wt. % salts can be explained by fluid interaction  
304 with gas hydrate (Fig 3). Fluorine has a low solubility in aqueous fluids and is retained by or  
305 incorporated into several marine minerals during diagenesis. In contrast, diagenesis releases  
306 considerable Br and I from the solid phase in organic-rich sediments to the fluid phase. It is  
307 usually assumed that Cl has a negligible concentration in the solid phase of marine sediment  
308 (Martin et al., 1993; Muramatsu et al., 2007; Gieskes and Mahn, 2007). However, the few data  
309 available for Cl in lithified sedimentary rock indicate surprisingly high Cl concentrations  
310 ranging up to ~1000's of ppm, which might be partly explained by the variable presence of salt  
311 derived from seawater or sedimentary pore waters (Table 2; John et al., 2011; Turekian and  
312 Wedepohl, 1961). Further data are therefore required to evaluate the significance of water  
313 soluble halogens in marine sediment and to improve the constraint on the Cl content of the  
314 solid phase. Water soluble halogens might be included in estimates of bulk silicate Earth  
315 concentrations, but removal of pore waters by sediment compaction suggests that sedimentary  
316 pore waters (and therefore salt in dry sediments) are not relevant for estimation of deep  
317 subduction budgets (Peacock, 1990).

318

319 **9.3 The oceanic crust-lithosphere and the scale of fluid infiltration**

320 As a first step toward evaluating the behaviour of halogens during alteration and metasomatism  
321 of the oceanic crust, it is desirable to review current knowledge concerning the structure of the  
322 oceanic crust and the scale of fluid infiltration.

323 It is now recognised that the character of the oceanic crust generated along the Earth's  
324 67,000 km long system of oceanic spreading centres varies as a function of spreading rate (Bird,  
325 2003; Dick et al., 2006; Snow and Edmonds, 2007). The classic 'Penrose' style of oceanic  
326 crust, as defined by the participants of the 1972 Penrose conference (Conference Participants,  
327 1972), which has a homogenous layered structure where sediments are underlain by pillow  
328 basalts, sheeted dykes, and layered intrusives, is only generated at fast spreading centres (>60  
329 mm/yr; Dick et al., 2006). In these cases, the rate of magma supply exceeds the rate of plate  
330 divergence and the seismic Moho at depths of 6-7 km represents a petrological transition from  
331 layered gabbro to peridotite (Fig 4; Dick et al., 2006).

332 In contrast, extremely heterogenous crust is generated at ultra-slow spreading centres,  
333 which have rates of divergence of <20 mm/yr, and account for more than 20,000 km of the  
334 global ridge system (Bird, 2003; Dick et al., 2003). In some cases, ultra-slow spreading centres  
335 are completely amagmatic and characterised by tectonic extension with hydrated ultramafic  
336 rocks (serpentinites) exposed on the seafloor (Dick et al., 2006; Snow and Edmonds, 2007). In  
337 other cases, a thin and/or patchy carapace of volcanic rock lies directly on top of layered  
338 intrusives or mantle peridotites (Fig 4; Dick et al., 2006) and the seismic Moho at depths of  
339 only 1-4 km could represent a hydration front between serpentine and mantle peridotite, as  
340 originally suggested by Hess (1962).

341 Finally, slow spreading ridges, such as the Mid-Atlantic Ridge, with rates of divergence  
342 of between 20 mm/yr and 60 mm/yr, are characterised by alternating segments of the two

343 crustal styles implying the Penrose model is inadequate for a large portion of the oceanic crust  
344 (Dick et al., 2006; Larsen et al., 2009; Snow and Edmonds, 2007).

345

### 346 ***9.3.1 Crustal permeability***

347 Pillow lavas and hyaloclastite breccias in seismic layer 2a of the oceanic crust have  
348 relatively high permeability ( $\sim 10^{-13}$  m<sup>2</sup>), meaning that the upper 500 m of the crustal basement  
349 enjoys good connectivity with cold seawater and is subject to low-temperature ‘brownstone’  
350 facies weathering at very high water/rock ratios (e.g. w/r > 100; Anderson et al., 1985; Fisher,  
351 1998). In situ borehole permeability measurements indicate permeability decreases to  $10^{-18}$ -  
352  $10^{-15}$  m<sup>2</sup> at greater depths, but numerical heat flow models imply that localised fracture  
353 generated permeabilities of up to  $10^{-9}$  m<sup>2</sup> control the effective permeability in the deeper crust  
354 (Fig 4; Anderson et al., 2012; Fisher, 1998; Fisher and Becker, 2000; Nehlig, 1994).  
355 Unlithified sediments represent a low permeability barrier to vertical fluid flow (Fig 4) and  
356 hydrothermal systems on the ridge flanks are therefore connected to seawater, and each other,  
357 through fractures exposed on basement outcrops (Anderson et al., 2012; Hutnak et al., 2008).

358

### 359 ***9.3.2 High temperature hydrothermal vent systems***

360 High temperature (350-400 °C) black smoker vent systems, where precipitation of Fe,  
361 Cu, and Zn sulphides generate vent chimneys and sulphide mounds, are found along mid-ocean  
362 ridges, back arc basin spreading centres and at intra-plate submarine volcanoes (Baker and  
363 German, 2004; Edmond et al., 1979; Hannington et al., 2011; Staudigel et al., 2004; Von Damm  
364 et al., 1985). The majority of high temperature hydrothermal fields at spreading centres occur  
365 on the ridge axes, but off-axis systems linked to crustal fractures are known at distances of up

366 to several km from the axis (Melchert et al., 2008; Rona et al., 1990; Zierenberg et al., 1995).  
367 The circulation of hydrothermal fluids is responsible for up to 80 % of the geothermal heat lost  
368 in these settings, meaning it is the major mechanism by which the oceanic crust cools (e.g.  
369 Williams et al., 1974).

370 Heat flow calculations and the distribution of hydrothermal plumes in the water column  
371 indicate that independent vent fields and associated ore deposits (e.g. hydrothermal outflow  
372 zones) occur at intervals of as little as 25 km along fast spreading centre ridge axes and as far  
373 apart as 200 km on slow spreading centre ridge axes (Baker, 2007; Hannington et al., 2011).  
374 Seawater is drawn into the oceanic crust to feed these systems through fractures, gaps between  
375 pillow lavas or dykes, and breccia zones over wide but poorly defined areas between the vent  
376 fields and on the ridge flanks (Anderson et al., 2012; Hutnak et al., 2008).

377 Seismic evidence for brittle deformation suggests that hydrothermal fluids penetrate to  
378 maximum depths of ~10 km on parts of the Mid-Atlantic Ridge (Glasby, 1998). The TAG  
379 hydrothermal field at 26° N on the Mid-Atlantic Ridge is situated above a 15 km long  
380 detachment fault that penetrates >7 km into the crust to near Moho depths (deMartin et al.,  
381 2007). Periodic reactivation of the fault has supplied heat to the overlying hydrothermal  
382 system and enabled sporadic hydrothermal activity over tens to hundreds of thousands of years  
383 in this area (Humphris and Cann, 2000; Kleinrock and Humphris, 1996; Tivey et al., 2003).

384 In comparison, seismic evidence suggests that hydrothermal fluids penetrate only ~3  
385 km into the fast spreading East Pacific Rise (Glasby, 1998). Melt lenses at depths of 1-3 km  
386 on the East Pacific Rise supply heat to the overlying hydrothermal system but represent a  
387 barrier to deeper fluid flow. The duration of hydrothermal activity is difficult to constrain but  
388 is commonly related to magmatism on fast spreading ridges, and individual vent fields are  
389 probably sustained over periods of only ten's to hundred's of years (Stakes and Moore, 1991).



390

### 391 ***9.3.3 Serpentinite hosted systems***

392           The Lost City Hydrothermal Field on the Atlantis Fracture Zone occurs 15 km from the  
393 Mid-Atlantic ridge axis at 30° N (Kelley et al., 2001). This system is hosted by ultramafic  
394 rocks and is characterised by carbonate vent chimneys and low temperature (40-90° C) alkaline  
395 fluids (pH 9-10) (Kelley et al., 2001; 2007). The alkalinity of the fluids and the presence of  
396 hydrogen, methane and abiogenic hydrocarbons are characteristics of fluids produced by  
397 serpentinisation of ultramafic lithologies (Kelley et al., 2007; Proskurowski et al., 2008). The  
398 discovery of this system was significant because it is driven by heat generated by exothermic  
399 serpentinisation reactions, rather than magmatism, and similar reactions could potentially drive  
400 numerous hydrothermal systems distal to ridge axes, implying a much higher level of seafloor  
401 hydrothermal activity than previously recognised (Kelley et al., 2001). Serpentinites are  
402 commonly exposed along transform faults and low angle detachments related to oceanic core  
403 complexes, providing evidence for widespread fluid activity at varying distance from oceanic  
404 spreading axes (Fryer, 2002).

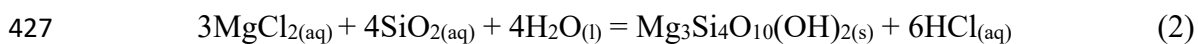
405           The slab bend formed immediately before subduction is now recognised as an  
406 additional site of important hydrothermal alteration (Fig 5). Seismic evidence suggests faults  
407 cut at least 20 km below the seafloor in this location, with the potential for large scale  
408 serpentinisation of the lithospheric mantle (Fig 5; Ranero et al., 2003). Heat flow  
409 measurements off shore Nicaragua and Central Chile indicate these areas are characterised by  
410 unexpectedly low heat flow consistent with heat loss by hydrothermal activity (Grevemeyer et  
411 al., 2005).

412

#### 413 **9.4 Black smoker vent fluid chemistry and halogens**

414 In comparison to seawater, high temperature black smoker vent fluids contain negligible Mg  
415 or  $\text{SO}_4^{2-}$  (dissolved sulphur is  $\text{S}^{2-}$ ), and are often depleted in U, P and F (Fig 6). In contrast,  
416 they are enriched in trace elements, dissolved  $\text{SiO}_2$  and contain 5-10 times more K and Ca  
417 relative to Na, than seawater (Fig 7). Typical vent fluids have pH of 3-4, maximum  
418 temperatures of close to 400 °C and salinities that range from 0.1 to 6 wt. % salts (Fig 8).

419 The composition of hydrothermal vent fluids results partly from chemical reaction of  
420 seawater with the oceanic crust and the mobilisation of trace elements and silica made possible  
421 by the high temperature of the fluid, acidity, and presence of the chloride ligand (Bischoff and  
422 Dickson, 1975; Humphris and Thompson, 1978; Seyfried and Bischoff, 1981). The take up of  
423 Mg into Mg-rich hydrous-silicate minerals, including smectite, chlorite, amphibole, and talc,  
424 is important because Mg-metasomatism is the primary source of vent fluid acidity and leads to  
425 extensive hydration of the crust (reaction 2; Bischoff and Dickson, 1975; Seyfried and Mottl,  
426 1982).



428  $\text{SO}_4^{2-}$  is removed from solution by reduction to sulphide and precipitation with Ca as anhydrite;  
429 Ca is released to the fluid by albitisation of plagioclase and the Ca/Na ratio of the fluid is  
430 subsequently controlled by plagioclase and epidote solid solution (Berndt et al., 1989).  
431 Potassium is incorporated into K-minerals at low temperature but it is released to the fluid at  
432 temperatures of >150 °C, which means most high temperature vent fluids have K/Cl ratios  
433 higher than seawater. The K/Cl ratio of the vent fluid is usually limited by the low K content  
434 of the basaltic crust, but high K/Cl ratios occur in the Manus basin vent fluids where more  
435 evolved K-rich rocks are present on the seafloor (Fig 7; Reeves et al., 2011).

436           The growth of Mg-rich hydrous minerals causes a finite increase in the salinity of  
437 hydrothermal fluids; however, this is only detectable at low water-rock ratios of <1 (e.g. Kelley  
438 and Robinson, 1990; Seyfried et al., 1986; Seyfried and Mottl, 1982). Therefore, the  
439 occurrence of vent fluids with salinities of less than seawater, and in some cases the dominance  
440 of vent fluids with lower than seawater salinity over many years of observation (Campbell et  
441 al., 1988), has been interpreted as strong evidence for phase separation and segregation of  
442 brines and vapours in submarine hydrothermal systems (Bischoff and Rosenbauer, 1989;  
443 Butterfield et al., 1997; Seyfried et al., 2003; Von Damm et al., 1997).

444

#### 445 ***9.4.1 Phase relations in the H<sub>2</sub>O-NaCl system***

446           The phase relations of sub-marine hydrothermal systems are strongly controlled by the  
447 presence of salts. Pure water exists as a homogenous supercritical fluid above its critical point  
448 (374 °C; 220 bars). In contrast, a critical curve extends beyond the critical point of pure H<sub>2</sub>O  
449 in any binary H<sub>2</sub>O-salt system, and the two-phase region is vastly expanded (Fig 9; e.g.  
450 Bischoff and Pitzer, 1989; Driesner and Heinrich, 2007). The critical point of seawater (407  
451 °C; 220 bars) lies on the critical curve of the H<sub>2</sub>O-NaCl system and joins the boiling curve to  
452 the condensation curve in Fig 9a (e.g. Bischoff and Pitzer, 1989; Bischoff and Rosenbauer,  
453 1984; Driesner and Heinrich, 2007). Sub-critical phase separation occurring below the critical  
454 point of seawater produces a small quantity of vapour, whereas super-critical phase separation  
455 occurring above the critical point of seawater produces a small quantity of brine (Fig 9).

456           The slope of the critical curve implies that phase separation will produce progressively  
457 more saline brines at higher pressures and temperatures deeper within the oceanic crust (Fig  
458 9). The salinity of brines also increases as the L-V isotherms are overstepped, such that at 500  
459 °C and 540 bars the first brine exsolved has a salinity of 28 wt. %, but further decompression

460 to 450 bars would yield a brine of 44 wt. % NaCl (points 1 and 2; Fig 9b). It is important to  
461 note that the salinities of the vapours and brines produced at different temperature and pressure  
462 conditions are controlled exclusively by the shape of the liquid-vapour envelope. For example  
463 at 500 °C and 450 bars, parental fluids with salinities of either 3.2 wt. % NaCl (seawater) or 10  
464 wt. % NaCl, would both exsolve into conjugate fluids with identical salinities, but at different  
465 proportions that can be estimated by the lever rule (point 2; Fig 9b).

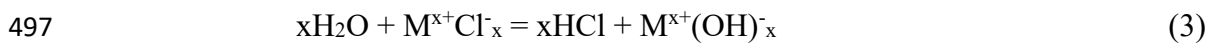
466 In addition to the well documented phenomena of liquid-vapour immiscibility,  
467 precipitation of hydrothermal-halite is possible under some circumstances (e.g. point 4; Fig 9).  
468 This is possible for seawater, which is approximated by the H<sub>2</sub>O-NaCl system (Fig 9), because  
469 hydrostatic pressures above spreading centres at typical water depths of 2000-2500 m are only  
470 ~200-250 bars and seawater heated above ~400 °C would separate into steam and halite (Fig  
471 9). Butterfield et al. (1997) presented photomicrographic evidence for halite coating glass  
472 surfaces and intergrown with TiO<sub>2</sub>, AlO(OH), and sphalerite, that was interpreted as evidence  
473 for precipitation of hydrothermal halite during high temperature interaction of seawater with  
474 seafloor lavas. The precipitation of hydrothermal halite has also been suggested as a possible  
475 cause of Br and Cl fractionation in some hydrothermal vent fluids (Berndt and Seyfried, 1997;  
476 Foustoukos and Seyfried, 2007). However, it should be noted that the vapour-salt field is  
477 probably restricted to much shallower depths in the multi-component salt systems that are  
478 relevant for hydrothermal fluids than in the H<sub>2</sub>O-NaCl system that is relevant for seawater  
479 (below).

#### 480 ***9.4.2 Complex salt systems and hydrolysis***

481 Hydrothermal vent fluids are better modelled in the ternary H<sub>2</sub>O-NaCl-CaCl<sub>2</sub> system  
482 than in the NaCl-H<sub>2</sub>O system (Vanko et al., 1988) because they have Ca/Na and K/Na ratios  
483 elevated by 5-10 times compared to seawater (Fig 10). The two phase field is even larger in

484 these complex salt systems than in the H<sub>2</sub>O-NaCl system. The critical curve for H<sub>2</sub>O-K/Cl is  
485 similar to that of H<sub>2</sub>O-NaCl, but the critical curve for H<sub>2</sub>O-CaCl<sub>2</sub> moves to significantly higher  
486 pressure at any given temperature than in the H<sub>2</sub>O-NaCl system (Fig 10; Bischoff et al., 1996;  
487 Driesner and Heinrich, 2007; Hovey et al., 1990). In addition, at temperatures of 400-450 °C,  
488 the vapour-salt field shrinks back from pressures of 180-250 bars in the H<sub>2</sub>O-NaCl system (that  
489 overlap the seafloor; Fig 10), to 130-170 bars in the H<sub>2</sub>O-KCl system and to as little as ~40-65  
490 bars in the H<sub>2</sub>O-CaCl<sub>2</sub> system (Fig 10; Driesner and Heinrich, 2007; Hovey et al., 1990; Keevil,  
491 1942; Ketsko et al., 1984).

492 In addition to the role of Cl as an important ligand for metal transport in hydrothermal  
493 solutions (e.g. Yardley, 2005), hydrolysis reactions in H<sub>2</sub>O-salt systems can have a significant  
494 influence on the pH of hydrothermal fluids (e.g. reaction 3; Bischoff et al., 1996; Seyfried et  
495 al., 1988; Seyfried and Bischoff, 1981). Hydrolysis reactions in binary salt systems have the  
496 general form:



498 The equilibrium lies to the left under Earth's surface conditions, meaning salt solutions have a  
499 neutral pH, but the equilibrium can be significantly shifted to the right under some crustal  
500 conditions. Bischoff et al. (1996) demonstrated that at temperatures of 350-500 °C hydrolysis  
501 is significantly more important in the CaCl<sub>2</sub>-H<sub>2</sub>O system than in the binary NaCl-H<sub>2</sub>O system.  
502 Fournier and Thompson (1993) reported that hydrolysis does not occur in the liquid-vapour  
503 region of the H<sub>2</sub>O-NaCl-KCl system, but that HCl is a significant component of the steam in  
504 equilibrium with halite in the vapour-salt region of the H<sub>2</sub>O-NaCl and H<sub>2</sub>O-NaCl-KCl systems.  
505 The varying degrees of hydrolysis in the different salt systems are related to the relative  
506 solubilities of the metal hydroxide produced by hydrolysis: Ca(OH)<sub>2</sub> has a low solubility

507 meaning it is removed from solution more efficiently than NaOH and as a result reaction 3 is  
508 pushed further to the right (Bischoff et al., 1996).

509 In nature the hydroxide component produced by hydrolysis reacts with silicates to form  
510 hydrous silicate minerals in the oceanic crust. For example, hydrolysis of  $MgCl_2$  leads to Mg  
511 being fixed in hydrous silicate minerals under prograde conditions as seawater is drawn into  
512 hydrothermal systems (reaction 2; Seyfried et al., 1988). The reactivity of Mg in the oceanic  
513 crust means that it is quickly removed from solution and Mg is not present in the hydrothermal  
514 fluids that reach the high temperature reaction zone above the magma chamber. In the absence  
515 of  $MgCl_2$ , hydrolysis of  $CaCl_2$  becomes the main acid generating reaction and is important in  
516 the hydrothermal upflow zones; hydrolysis of NaCl can be locally important in zones of Na  
517 metasomatism (Seyfried et al., 1988). The generation of acidity by hydrolysis reactions is  
518 important because it enables mobilisation of heavy metals from seafloor lithologies (Seyfried  
519 and Bischoff, 1981). Furthermore, HCl partitions into the vapour produced by phase separation  
520 (Fig 10; Bischoff et al., 1996), meaning segregation of vapours and brines enables discrete  
521 zones of alkali or acid metasomatism to develop in different parts of the oceanic crust, or waves  
522 of acid metasomatism to pass through a hydrothermal system (Kigai and Tagirov, 2010).

523

#### 524 ***9.4.3 Halogen abundance ratios in vent fluids***

525 There has been considerable interest in the relative abundances of halogens in hydrothermal  
526 vent fluids. The existing data show vent fluids have F concentrations ranging from ~0.1 to 7  
527 ppm, compared to the seawater value of 1.3 ppm F, and that F varies independently of Cl with  
528 vent fluid F/Cl ratios varying by almost two orders of magnitude around the seawater value  
529 (Fig 11a; Edmond et al., 1979; Gieskes et al., 2000; Gieskes et al., 2002; James et al., 2014;  
530 Mottl et al., 2011; Reeves et al., 2011; Von Damm et al., 1985). The reported variation in F

531 fits well with experimental studies that demonstrate F is removed from solution as seawater  
532 interacts with basalt and is heated from 150 to 250 °C, but re-enters solution with further  
533 heating to 300 °C (Seyfried and Ding, 1995). Fluorine is incorporated into Mg-carbonate (cf.  
534 Fig 1) and hydrous minerals at low temperature but the direction of hydroxyl-fluoride and  
535 carbonate-fluoride exchange reactions reverses at high temperature when the speciation of  
536 dissolved F changes from  $F^-_{(aq)}$  to  $HF_{(aq)}$ , which reduces the chemical activity of the  $F^-$  anion  
537 (Seyfried and Ding, 1995). Consequently the experimental studies imply that while magmatic  
538 F might be mobilised in deeper parts of the crust as  $HF_{(aq)}$ , it is likely that seawater  $F^-_{(aq)}$  is  
539 removed from solution during heating and is not advected deeply into the crust (Seyfried and  
540 Ding, 1995). The co-depletion of some hydrothermal fluids in P as well as F suggests that  
541 precipitation of fluorapatite is also important (Fig 6; Gieskes et al., 2002).

542 A number of studies have investigated Br in hydrothermal fluids and demonstrated that  
543 the Br/Cl ratio of the vent fluids is usually within 10 % of the seawater value and that it does  
544 not vary systematically as a function of salinity (Fig 11b). Furthermore, conjugate vapours and  
545 brines from vent F at 9°16' N on the East Pacific Rise (Von Damm et al., 1997) and Milos  
546 Island in the Hellenic Arc (Wu et al., 2012) have similar Br/Cl ratios (Fig 11b). Taken together  
547 these data strongly suggest that the Br/Cl ratio is not strongly or systematically altered by  
548 liquid-vapour phase separation in the majority of hydrothermal systems investigated (Fig 11b).  
549 This conclusion is consistent with experiments on NaCl solutions that show no systematic  
550 fractionation of Br and Cl during sub-critical phase separation (Berndt and Seyfried, 1997).  
551 Experiments under other conditions have shown fractionation of Br relative to Cl into either  
552 vapours or brines during phase separation (see Berndt and Seyfried, 1990; Foustoukos and  
553 Seyfried, 2007; Liebscher et al., 2006). However, the results from the different laboratories are  
554 not in agreement and the available Br/Cl data summarised for vent fluids in Fig 11 are more

555 easily explained by the conservation of Br/Cl during phase separation with unusual Br/Cl ratios  
556 of fluids in specific settings being explained by fluid-rock reactions (below).

557         The unusually high Br/Cl ratios in fluids from a small number of vents (Fig 11b) can  
558 be explained by fluid interaction with sedimentary material, because where Br/Cl and I/Cl data  
559 are both available these ratios co-vary in a manner comparable to that observed for sedimentary  
560 pore waters (Fig 11c; Campbell and Edmond, 1989; Campbell et al., 1994; Gieskes et al., 2002;  
561 Kawagucci et al., 2011; Mottl et al., 2011; You et al., 1994). Furthermore, I concentrations are  
562 correlated with NH<sub>4</sub> and other sediment-derived components in these fluids (Campbell et al.,  
563 1994; You et al., 1994). Note that limited data are available for I or F in vent fluids and halogen  
564 data for sedimentary pore fluids with mantle-like <sup>3</sup>He/<sup>4</sup>He signatures, which are believed to  
565 represent hydrothermal fluids from beneath the Escanaba Trough hydrothermal system (Hole  
566 1038B-H; Ishibashi et al., 2002; James et al., 1999), are included in Fig 11 as light blue symbols  
567 (Gieskes et al., 2000; 2002). These ‘hydrothermal pore fluids’ have Br/Cl and I/Cl values  
568 overlapping the range reported for Escanaba Trough vent fluids (Fig 11c; Campbell and  
569 Edmond, 1989; Campbell et al., 1994; You et al., 1994).

570         Unusually low Br/Cl ratios are restricted to a few locations between 9° and 10° N on  
571 the East Pacific Rise (Oosting and Von Damm, 1996) and Milos Island in the Hellenic Arc (Fig  
572 11b; Wu et al., 2012). It is possible that vent fluids acquired low Br/Cl ratios in these settings  
573 by fluid interaction with sedimentary halite or by leaching glassy magmatic rocks that are  
574 typically characterised by Br/Cl of less than seawater (see mantle field in Fig 11c; Jambon et  
575 al., 1995; Kendrick et al., 2013a; Schilling et al., 1980). Similarly low Br/Cl ratios have been  
576 reported for unusual sediment pore waters that have interacted with glassy volcanoclastic rocks  
577 in the Aoba Basin of the New Hebrides convergent margin (Martin, 1999). Strongly altered,  
578 palagonitised glasses can also be depleted in Cl and Br relative to pristine glasses (Fig 12;



579 Kendrick et al., 2015) confirming that these elements are mobilised during low temperature  
580 alteration of glass.

581 Finally, the fact that most vent fluids have Br/Cl ratios within 10 % of seawater (Fig  
582 11) implies that in most cases, fluid-rock ratios are sufficiently high that Br and Cl behave  
583 conservatively in hydrothermal vent fluids and are not significantly altered by reaction with  
584 mafic lithologies (Br concentrations are altered by interaction with sediments; Fig 3;  
585 Muramatsu et al., 2007; Price and Calvert, 1977). In contrast, leaching of Cl>Br from glassy  
586 rocks is possible and has the potential to lower the Br/Cl ratio of a fluid. Furthermore, at low  
587 water-rock ratios, precipitation of OH>Cl>Br in Fe/Mg-hydroxy chlorides, or amphibole, has  
588 the potential of increasing a fluid's salinity and Br/Cl ratio (Kendrick et al., 2015b; Seyfried et  
589 al., 1986; Svensen et al., 1999, 2001; Vanko, 1986). Therefore, it should not be assumed that  
590 Br and Cl behave conservatively under all hydrothermal conditions.

591

## 592 **9.5 Fluids in the deeper crust**

593 Evidence for the nature of fluids in deeper parts of the oceanic crust comes from mineral  
594 alteration (Gillis and Meyer, 2001; Vanko, 1986), fluid inclusions (Fig 13; Kelley et al., 1993;  
595 1992; Kendrick et al., 2015b; Nehlig, 1991; Vanko, 1988; Vanko et al., 1992), and studies of  
596 magmatic glass that contain assimilated halogens (below; Kendrick et al., 2013a; 2015a). Fluid  
597 inclusions have been investigated in minerals such as quartz, anhydrite, sphalerite, epidote,  
598 amphibole, and chlorite from a number of dredges and ophiolites. These include samples from  
599 within and just below the vent chimney all the way down to upper amphibolite facies  
600 metagabbros from layer 3 of the oceanic crust (Castelain et al., 2014; Juteau et al., 2000; Kelley  
601 and Delaney, 1987; Kelley and Robinson, 1990; Kelley et al., 1992, 1993; Lécuyer et al., 1999;  
602 Nehlig, 1991; Nehlig and Juteau, 1988; Vanko, 1986; 1988; 1992; 2004).

603 Collectively these studies demonstrate the predominance of low salinity Na-Ca-Cl  
604 fluids throughout the oceanic crust that are broadly similar to vent fluids. For example, Nehlig  
605 (1991) reported that more than 95% of the fluid inclusions examined in samples taken from  
606 crustal sections through the Semail and Trinity ophiolites of Oman and California, and in  
607 samples from the Gorringe Bank of the East Pacific Rise, had salinities within 1 wt. % of  
608 seawater. However, in addition to the dominant fluid inclusions with salinities of 0.1-6 wt. %,  
609 which are similar to vent fluids, fluid inclusions with extreme Ca enrichment ( $\text{Ca/Na} = 1$ ),  
610 which is stronger than known from vent fluids (Fig 7), have been reported (Vanko et al., 1992)  
611 and brine inclusions with salinities of up to 50 wt. % salts appear to be a common minor  
612 component at all levels of the oceanic crust (Fig 13; Juteau et al., 2000; Kelley and Delaney,  
613 1987; Lécuyer et al., 1999; Vanko, 1988; 2004; Aranovich et al., 2015).

614 Brine inclusions with salinities of  $\sim 30$  wt. % salts have been reported in the vent  
615 chimneys of several systems in the Lau Basin and within a few hundred metres of the seafloor  
616 beneath the Pacmanus system, demonstrating that high salinity brines are not restricted to deep  
617 parts of the oceanic crust (Lécuyer et al., 1999; Vanko et al., 2004). However, high salinity  
618 brine inclusions are most commonly reported from deeper amphibolite settings (Vanko, 1988;  
619 Kendrick et al., 2015b) and above newly emplaced gabbroic intrusions (Kelley and Delaney,  
620 1987) or plagiogranites that form in the roof zones of crustal magma chambers (Kelley and  
621 Robinson, 1990; Nehlig, 1991; Vanko et al., 1992). In many cases the brine inclusions co-exist  
622 with more abundant low salinity vapour inclusions that provide evidence for their origin by  
623 phase separation (e.g. Juteau et al., 2000; Kelley and Delaney, 1987; Vanko, 1988). The  
624 dominance of vapour inclusions is the expected result of seawater undergoing phase separation  
625 (e.g. point 2 in Fig 9; Bischoff and Pitzer, 1989). However, the vapour inclusions can have  
626 salinities that are even greater than seawater suggesting complex multi-stage histories and/or  
627 input of a magmatic component.

628           In some cases, brine inclusions dominate samples recovered from layer 3 of the crust.  
629   These inclusions have been interpreted as brines that have been segregated from their conjugate  
630   vapours, but their origin by phase separation cannot be proven (Kelley and Robinson, 1990;  
631   Vanko et al., 1992). The fluid inclusion evidence for possible segregation of brines in layer 3  
632   of the oceanic crust is significant because brine segregation and double diffusive convection of  
633   fluids in the oceanic crust has previously been invoked to explain the predominance of fluids  
634   with lower than seawater salinity emitted from vents on the seafloor (Fig 14; Bischoff and  
635   Rosenbauer, 1989). It is suggested the brines would be segregated because of the different  
636   wetting properties and buoyancies of vapours and brines in a micro-scale fracture network.  
637   Buoyant vapours would be preferentially lost to the overlying hydrothermal system, whereas  
638   dense brines could be trapped in the lower crust. If correct, this model implies brines generated  
639   by multiple episodes of phase separation gradually accumulate in the deeper crust and they are  
640   implied to have long residence times in the crust at very low effective water-rock ratios (Fig  
641   14). The ultimate fate of brines within this model is unknown but brines might eventually be  
642   flushed out of the crust by advection of more typical low salinity fluids in the waning stages of  
643   hydrothermalism or they might be transported laterally and leak out of the ridge flanks away  
644   from the vents (Bischoff and Rosenbauer, 1989). In addition, a portion of these brines could  
645   be assimilated by magmas driving the hydrothermal system (Kendrick et al., 2013a; 2015) or  
646   involved in flux melting and the genesis of plagiogranites (Aranovich et al., 2010, 2015).

647           A major uncertainty related to the brine fluid inclusions is whether they originate purely  
648   from evolved seawater or include a component derived from late-stage magmatic fluids.  
649   Magmatic fluids exsolved from basic rocks are dominated by CO<sub>2</sub> with a low salinity aqueous  
650   component (Dixon et al., 1995; Webster et al., 1999). However, more saline fluids might  
651   sometimes be exsolved from evolved intrusive rocks such as plagiogranites in magma chamber  
652   roof zones (Kelley and Robinson, 1990; Kelley et al., 1992). If magmatic fluids enter the two-

653 phase field, their salinity depends on the shape of the liquid-vapour envelope in the relevant  
654 water-salt system (e.g. Figs 9 and 10), meaning that it is not possible to infer the source of the  
655 fluid (e.g. seawater or magmatic) from the measured salinity. Vanko et al. (1992) suggested  
656 that a minor magmatic component could be present in high salinity CO<sub>2</sub>-bearing fluid inclusion  
657 assemblages from the Oceanographer Transform, but favoured an origin entirely from evolved  
658 seawater for brines trapped without accompanying CO<sub>2</sub> on the Mathematician Ridge (Vanko,  
659 1988; 1992; Kendrick et al., 2015b). Reeves et al. (2011) suggested that unusually high F/Cl  
660 ratios in Manus Basin vent fluids could result from the input of magmatic volatiles (Fig 11).

661

### 662 *9.5.1 Halogens in brines and assimilation by magmas*

663 The systematics of Br/Cl, I/Cl, and F/Cl in brine inclusions can be inferred from two  
664 separate lines of evidence. Kendrick et al. (2015b) investigated halogens and noble gases in  
665 high salinity brine and vapour fluid inclusions in six quartz/epidote veins from the  
666 Mathematician Ridge of the NE Pacific using a bulk extraction technique. The fluid inclusions  
667 in all the veins were shown to have a similar range of Br/Cl and I/Cl irrespective of the relative  
668 proportions of brine and vapour fluid inclusions (Fig 15). In addition, Br/Cl was not correlated  
669 with Ar/Cl, which is strongly altered by phase separation (Kendrick et al., 2015b). Taken  
670 together these data suggest that Br/Cl and I/Cl were not fractionated during phase separation  
671 of Mathematician Ridge fluids, consistent with the behaviour of Br/Cl in vent fluids (section  
672 9.4.3). On average the Mathematician Ridge fluids have Br/Cl ~20% higher than seawater and  
673 I/Cl intermediate of seawater and the mantle (Fig 15; Kendrick et al., 2015b). These  
674 compositions were attributed to mixing halogens introduced by seawater with halogens  
675 mobilised from the crust and preferential exclusion of Br and I relative to Cl from amphibole  
676 crystallised at low water rock ratios (Fig 15; Kendrick et al., 2015b). Proton Induced X-ray

677 Emission (PIXE) has been used to analyse some individual brine inclusions from the  
678 Mathematician Ridge, Oceanographer Transform and Oman ophiolite (Juteau et al., 2000;  
679 Vanko et al., 2001). The majority of the fluid inclusions investigated by PIXE are indicated to  
680 have Br/Cl close to or above seawater, but the precision of the analyses is low (Juteau et al.,  
681 2000; Vanko et al., 2001).

682         The second constraint on the halogen composition of high salinity brines in the oceanic  
683 crust comes from recent studies of magmatic glass (Kendrick et al., 2013a; 2015a). It has long  
684 been recognised that some magmatic glasses contain ‘excess Cl’ introduced by the assimilation  
685 of seawater-derived components (Michael and Cornell, 1998; Michael and Schilling, 1989).  
686 Most workers have favoured the assimilation of hydrothermally altered crust to account for  
687 excess Cl. However, plotting the H<sub>2</sub>O/Cl and K/Cl ratios of all known glasses, identified as  
688 containing excess seawater-derived Cl (Coombs et al., 2004; Freund et al., 2013; Kent et al.,  
689 1999ab; 2002; le Roux et al., 2006; Lytle et al., 2012; Wanless et al., 2010), shows that Cl is  
690 introduced into these melts by high salinity brines (e.g. Fig 16; Kendrick et al., 2013a). This  
691 is shown by the data in Fig 16 which extend from a range of compositions representative of the  
692 mantle to converge on a single component with very low ratios of H<sub>2</sub>O/Cl, K/Cl, and F/Cl that  
693 are characteristic of a Na-Ca-K-Cl brine with salinity of >50 wt % salts (Fig 16; Kendrick et  
694 al., 2013a; 2015a). In contrast, altered crustal material would have much higher H<sub>2</sub>O/Cl (Ito  
695 et al., 1983). The Br and I data available for glasses, affected by brine assimilation from the  
696 NW part of the Lau Basin, the Galapagos, and Samoa, define coherent mixing trends with K,  
697 Cl, and H<sub>2</sub>O, demonstrating that the assimilated brines are characterised by Br/Cl and I/Cl  
698 ratios a few 10’s of percent higher than seawater (Figs 15 and 16), that are very similar to the  
699 range of compositions determined for Mathematician Ridge fluid inclusions (Kendrick et al.,  
700 2015b).

701           The brine assimilation data are significant because: i) some of the glasses affected have  
702 high concentrations of H<sub>2</sub>O and CO<sub>2</sub>, which demonstrate that assimilation must have occurred  
703 at depth in crustal magma chambers rather than on the seafloor (Coombs et al., 2004; Kendrick  
704 et al., 2013a; le Roux et al., 2006), and ii) the data provide evidence that seawater-derived  
705 brines, with Br/Cl and I/Cl distinct from the mantle, not only penetrate the lower crust but come  
706 into direct contact with, and are assimilated by crustal magmas (Fig 16). Mass balance  
707 calculations suggest the affected magmas from the NW part of the Lau Basin, the Galapagos,  
708 and Samoa assimilated up to 0.5 % of their total mass in brine which introduced 0-70 % of  
709 their total Cl and 0-30 % of their total H<sub>2</sub>O (Kendrick et al., 2013a; 2015). Therefore,  
710 assimilation of brines generated in hydrothermal systems can alter the concentrations of  
711 halogens and relative abundance ratios (F/Cl, Br/Cl and I/Cl) of newly forming crust (e.g.  
712 magma), even before the new crust has been hydrothermally altered. In addition, the ductile  
713 zone, surrounding the magma chambers, is not a complete barrier to assimilation of seawater-  
714 derived volatiles.

715

## 716 **9.6 Halogens in altered oceanic crust and lithosphere**

717 A relatively small number of studies have investigated the bulk halogen content of the altered  
718 ocean crust with the majority of studies focused on Cl (Barnes and Cisneros, 2012; Bonifacie  
719 et al., 2007; Chavrit et al., 2016; Floyd and Fuge, 1982; Ito and Anderson, 1983; Ito et al.,  
720 1983; Kendrick et al., 2015b; Magenheim et al., 1995; Sano et al., 2008). The earliest estimates  
721 for whole rock Cl concentration were made by electron microprobe measurements of Cl in  
722 individual mineral phases, followed by estimation of the modal abundances of the minerals in  
723 the rock (Ito et al., 1983). Major problems with this approach are that intra-granular Cl and  
724 fluid inclusion hosted Cl, which can account for 100-200 ppm Cl in the bulk sample (Kendrick

725 et al., 2015b), or Cl present in volumetrically minor phases such as Fe hydroxychlorides are  
726 not included in the analysis. In addition, although detection limits of better than 50 ppm Cl can  
727 be achieved with sufficiently long counting times (e.g. Michael and Cornell, 1998) most  
728 minerals have Cl concentrations of less than the typical 100-300 ppm detection limits for Cl  
729 achieved by routine electron microprobe analysis.

730         Direct measurements of Cl have been achieved by various instrumental neutron  
731 activation techniques that provide modest  $2\sigma$  precision of 15-20 % (Sano et al., 2008) or 200  
732 ppm Cl (Barnes and Cisneros, 2012), and have the significant advantage of requiring minimal  
733 sample processing.

734         Direct measurements of F, Cl, and I have also been achieved by digestion of powders  
735 and spectrophotometry (Floyd and Fuge, 1982) and more recently by combining  
736 pyrohydrolysis for halogen extraction from powders with ion chromatography for F and Cl  
737 analysis (Bonifacie et al., 2007; John et al., 2011; Magenheim et al., 1995; Sharp and Barnes,  
738 2004) and ICP-MS for Br and I analysis (John et al., 2011). These techniques can provide  
739 accurate results with internal precision of better than 5%. However, Bonifacie et al. (2007)  
740 demonstrated that Cl yields vary between labs with yields as low as 40 % in some of the early  
741 studies, implying that significant fractionation of halogens during extraction is possible.

742         Kendrick et al. (2011, 2013a, 2015) and Chavrit et al. (2016) employed ‘the noble gas  
743 method’ for analysis of Cl, Br, I, and K whereby neutron irradiation is used to generate noble  
744 gas proxy isotopes that can be precisely measured by noble gas mass spectrometry (Böhlke and  
745 Irwin, 1992; Johnson et al., 2000; Kendrick, 2012). This technique combines the advantages  
746 of neutron activation analysis, by avoiding wet chemical extraction of halogens (or K), with  
747 high internal precision of ~1-2 %.

748 Finally, the external precision of all methods is limited by the availability of well  
749 characterised standards for Br and I (Kendrick, 2012; Kendrick et al., 2013a; Marks et al.,  
750 2016). In addition, some differences between laboratories could be introduced by washing  
751 procedures, which might completely remove water soluble components from powdered  
752 samples. Water soluble halogens are especially important in marine sediments (Turekian and  
753 Wedepohl, 1961) and serpentinites (e.g. Sharp and Barnes, 2004).

754

### 755 ***9.6.1 Mineralogy and Cl content of oceanic crust***

756 The altered oceanic crust comprises relict glass and nominally anhydrous minerals typical of  
757 basalts and gabbros (e.g. plagioclase, pyroxene and olivine) and their hydrous alteration  
758 products. Parts of the crust that have interacted with cold seawater contain clay minerals  
759 (smectites including montmorillonite, and saponite), zeolites, and Fe-hydroxides. Glassy rocks  
760 present in hyaloclastites in Layer 2a of the crust can be extensively replaced by palagonite,  
761 which is defined as a heterogenous mixture of clays, zeolite, and oxides (Staudigel et al., 2008;  
762 Staudigel and Hart, 1983; Stroncik and Schmincke, 2002). At temperatures of 200 to 300°C,  
763 prehnite, pumpellyite, and chlorite are important. Actinolite, tremolite, albite, epidote, and  
764 sphene become important at >300 °C, and hornblende and phlogopite can be important at >400  
765 °C (Alt and Honnorez, 1984; Bideau et al., 1991; Talbi et al., 1999). In addition, a number of  
766 minerals, including carbonate and quartz, form over wide temperature ranges. The polymorphs  
767 of serpentine (chrysotile, lizardite, and antigorite) form in olivine-rich rocks between 100 and  
768 500 °C (Bideau et al., 1991) and talc forms by silica metasomatism under all prograde  
769 conditions (Seyfried et al., 1988). Typical water contents and what is known about the halogen  
770 contents of some common alteration minerals are summarised in Table 4.

771



### 772 **9.6.2 Low temperature seawater alteration**

773 Clay minerals contain a lot of water and significant F, but typically very little Cl (Table 4). For  
774 example smectites contain 5-15 wt. % H<sub>2</sub>O and the smectite veins analysed by Magenheim et  
775 al. (1995) had 150-400 ppm F but only ~20 ppm Cl. Kendrick et al. (2014) reported that  
776 palagonite crusts on Samoan glass contain 35 ppm Cl which represented a 97% depletion  
777 compared to the pristine glass (Fig 12). Although it is usually assumed that Cl is introduced  
778 into the oceanic crust during hydrothermal alteration, the very low Cl content of these clay  
779 minerals and palagonite demonstrates that parts of the oceanic crust could be depleted in Cl  
780 during low temperature alteration. Alternatively, halogens might be remobilised on a local  
781 scale (Floyd and Fuge, 1982), with for example, Cl released during clay alteration taken up by  
782 Fe-hydroxy chlorides (Table 4; Seyfried et al., 1986).

783 In comparison to Cl and F, even fewer data are available for Br or I. The palagonite  
784 investigated by Kendrick et al. (2015) was less depleted in Br, than Cl, and it was enriched in  
785 I relative to pristine glass. Chavrit et al. (2016) also demonstrated I enrichment in some clay-  
786 bearing samples of altered basalt. Therefore parts of the crust could be enriched in I relative to  
787 unaltered crust, both relative to Cl and in absolute terms (eg. high I and high I/Cl). Iodine could  
788 be trapped in altered ocean crust preferentially relative to Cl if it is adsorbed onto clay minerals  
789 (Claret et al., 2010; Montavon et al., 2014) or zeolites, which are micro-porous adsorbants.  
790 Alternatively, I is a biophilic element and there is growing evidence that microbes are involved  
791 in some styles of glass alteration (Alt and Mata, 2000; Fisk et al., 1998; Kruber et al., 2008;  
792 Staudigel et al., 2008; Stroncik and Schmincke, 2002) and alteration of some minerals  
793 (Ivarsson et al., 2008). Kruber et al. (2008) reported that palagonite formed by the bio-  
794 alteration of glass can contain up to 1 wt. % organic C ( $\delta^{13}\text{C} = -22 \text{‰}$ ). If the microbes  
795 responsible for this alteration have an I/C<sub>organic</sub> similar to plankton (0.0002-0.002; Bobrov et  
796 al., 2005; Iwamoto and Shiraiwa, 2012; Martin et al., 1993; Price and Calvert, 1977) this would

797 imply that exceptionally high I concentrations of ~2-20 ppm might be expected in biogenic  
798 palagonite.

799 In summary, low temperature alteration of the crust leading to hydration and formation  
800 of clays causes a finite increase in fluid salinity and some remobilisation of heavy halogens  
801 from the crust. However, because this alteration takes place at very high water-rock ratios the  
802 effects are difficult to discern in alteration fluids (section 5.4). Low temperature alteration of  
803 mafic lithologies, either by biological processes or by adsorption of I onto reactive minerals,  
804 might be significant for the marine I cycle (cf. Leblanc et al., 2006).

805

### 806 ***9.6.3 High temperature hydrothermal alteration***

807 Amphibole and serpentine are usually the only minerals in which Cl (and more rarely  
808 F) can be detected by electron microprobe. Other hydrous minerals such as prehnite,  
809 pumpellyite, chlorite and epidote are assumed to contain <100 ppm Cl but remove water from  
810 the system implying that they cause a finite increase in the salinity of alteration fluids. In  
811 addition to mineral matrices, a number of minerals can be important hosts of fluid inclusions.  
812 Fluid inclusions are often estimated to account for up to 1 vol. % of the coarse minerals with  
813 abundant inclusions. If these fluid inclusions trapped fluids with average salinities and  
814 densities similar to seawater, the fluid inclusions can be estimated to contribute up to 70 ppm  
815 Cl and 250 ppb Br but negligible F or I toward the mineral's bulk composition (Table 4). In  
816 comparison, Kendrick et al. (2015b) reported bulk halogen concentrations of 100-200 ppm Cl,  
817 300-600 ppb Br and 4-20 ppb I for fluid inclusions bearing vein minerals from the  
818 Mathematician Ridge.

819           The concentrations of F and Cl in amphiboles within the oceanic crust are extremely  
820 variable ranging from concentrations of 10's of ppm Cl and 100's ppm F in igneous amphibole  
821 up to wt. % levels of Cl in late-stage hydrothermal veins (Fig 17; Cortesogno et al., 2004; Gillis  
822 and Meyer, 2001; Jacobson, 1975; Nehlig and Juteau, 1988; Vanko, 1986). Actinolite, present  
823 under greenschist facies conditions, generally contains <500 ppm Cl (Vanko, 1986), which is  
824 consistent with the concentration range of 100-300 ppm expected to result from hydration by  
825 fluids with seawater salinity (Cortesogno et al., 2004; Kendrick et al., 2015b). In contrast,  
826 amphibolite grade hornblendes contain hundreds to thousands of ppm Cl (Cortesogno et al.,  
827 2004; Ito and Anderson, 1983; Nehlig and Juteau, 1988; Prichard and Cann, 1982; Tribuzio et  
828 al., 2014; Vanko, 1986; Silantyev et al., 2008). The variability of amphibole Cl concentrations  
829 under amphibolite conditions could reflect equilibration with segregated vapours and brines  
830 produced by phase separation of seawater that is heterogeneously distributed through this part  
831 of the crust (Cortesogno et al., 2004). Amphiboles with 1 to 6 wt. % Cl have been reported  
832 from several locations but are always a volumetrically minor component of the rock, which is  
833 commonly associated with late-stage veins and/or mylonites (Bideau et al., 1991; Honnorez  
834 and Kirst, 1975; Jacobson, 1975; Vanko, 1986). The effect of hydrothermal alteration is to  
835 introduce seawater Cl and redistribute igneous Cl and F between a growing number of  
836 amphiboles. As a result, amphiboles formed during progressive hydrothermal alteration are  
837 distinguished from igneous amphiboles by progressively higher Cl contents and Cl/Na ratios,  
838 and lower F/Cl ratios (Fig 17; Coogan et al., 2001; Mevel, 1988).

839           Crystal chemistry exerts an important control on amphibole halogen concentration. For  
840 example, the negative correlation between F/Cl and Cl in Fig 17 results in part from F and Cl  
841 competing to occupy the same site in amphibole. It has long been assumed that the large Br<sup>-</sup>  
842 and I<sup>-</sup> anions would be preferentially excluded from amphibole relative to Cl<sup>-</sup> and F<sup>-</sup> (Svensen  
843 et al., 1999; 2001), and this has recently been confirmed by the analysis of amphibole and

844 related fluid inclusions in amphibolites and metagabbros from the Mathematician Ridge  
845 (Kendrick et al., 2015b).

846 In addition to crystal chemistry, it is now generally agreed that high Cl amphiboles can  
847 only form when the chemical activity of Cl is high and the chemical activity of H<sub>2</sub>O is low,  
848 such as occurs in the presence of saline fluids (Kullerud and Erambert, 1999; Markl and  
849 Bucher, 1998; Vanko, 1986). Therefore, Cl-rich amphiboles do not provide a mechanism for  
850 reducing fluid salinity; rather, they provide evidence for the presence of high salinity fluids in  
851 the crust.

852 If phase separation is the major control on fluid salinity (Kelley and Delaney, 1987;  
853 Vanko, 1988), the increase in amphibole Cl content from greenschist to amphibolite facies can  
854 be interpreted as evidence for efficient segregation of brines and vapours and support for the  
855 idea that brines are preferentially stored in the deeper crust (e.g. Fig 14). However, while it  
856 has been recognised that crustal hydration can lead to appreciable increases in fluid salinity,  
857 the effect of 'drying up' or 'fluid desiccation' on salinity has not been evaluated within the  
858 context of the oceanic crust. For example, Kelley and Delaney (1987) suggest that formation  
859 of hydrous minerals could increase seawater salinity by a factor of two but favoured phase  
860 separation in the generation of ultra-saline brines. In contrast to this, it is well known that at  
861 water/rock ratios of less than 0.1-0.01 'drying up' leads to substantial increases in the  
862 concentration of all dissolved components (Reed, 1997). Furthermore, desiccation of  
863 metamorphic fluids is implicated in the generation of Cl-rich amphiboles and metamorphic salt  
864 in granulites in northern Norway, which provides strong evidence for the generation of ultra-  
865 saline fluids (up to 100 % salt) by this process in some settings (Kullerud and Erambert, 1999;  
866 Markl and Bucher, 1998). The high Cl content of amphibolite facies amphiboles can therefore  
867 also be interpreted as indicating fluid/rock ratios approach zero at the limit of the seafloor  
868 hydrothermal system (cf. Fig 14).

869           The relative importance of phase separation and ‘drying up’ might be tested in future  
870 studies of Cl, Br, and I in fluid inclusions and minerals. As Br and I are excluded from  
871 amphibole relative to Cl (Kendrick et al., 2015b), drying up should produce fluids with very  
872 high Br/Cl and I/Cl ratios (Svensen et al., 2001). Whereas because Br/Cl does not appear to be  
873 strongly fractionated by phase separation (Fig 11), phase separation might yield brines with  
874 Br/Cl and I/Cl much closer to seawater values (Kendrick et al., 2015b). This line of reasoning  
875 suggests that phase separation was the dominant process responsible for the generation of  
876 brines in the Mathematician Ridge hydrothermal system (Kendrick et al., 2015b) and brines  
877 assimilated by magmas which are all inferred to have Br/Cl ratios of only slightly higher than  
878 seawater (Fig 15; Kendrick et al., 2013a; 2015a).

879

#### 880 ***9.6.4 The bulk halogen content of the oceanic crust***

881 Sano et al. (2008) sampled core from Hole 1256D drilled in the Eastern Pacific at intervals of  
882 <50 m, over more than 1000 m of core, providing high density Cl concentration data that show  
883 a broad increase in Cl as a function of depth in this hole (Fig 18). Four additional studies have  
884 investigated Cl and Cl isotopes in seven different cores drilled in the Pacific, Atlantic, and  
885 Indian Oceans but sampling within each core is at a much lower density (Barnes and Cisneros,  
886 2012; Bonifacie et al., 2007; Chavrit et al., 2016; Magenheim et al., 1995). These studies  
887 show similar Cl concentration ranges as observed in Hole 1256D, in which low temperature  
888 alteration has a median Cl concentration of 160 ppm and high temperature alteration has a  
889 median concentration of 360 ppm Cl, but individual samples contain as little as 11 ppm or as  
890 much as 2000 ppm Cl (Fig 18; Barnes and Cisneros, 2012; Bonifacie et al., 2007; Chavrit et  
891 al., 2016; Magenheim et al., 1995; Sano et al., 2008). These studies indicate that the real  
892 concentration of Cl in the oceanic crust is several times higher than was initially estimated (50  
893  $\pm$  25 ppm Cl) on the basis of electron microprobe data (Ito et al., 1983).

894           Unfortunately, because crustal lithologies have extremely variable Cl concentrations  
895 (e.g. 200-1200 ppm Cl at 1500 m in Hole 1256D; Fig 18), the low density of data available  
896 from the majority of IODP holes means that it is difficult to assess if the broad increase in Cl  
897 observed with depth in Hole 1256D (Fig 18; Sano et al., 2008) is a general feature of the oceanic  
898 crust (cf. Barnes and Cisneros, 2012). However, the following observations suggest that Cl  
899 concentrations are likely to increase with depth: i) Cl and Br are mobilised into the fluid during  
900 alteration of glass (Fig 12; Floyd and Fuge, 1982; Kendrick et al., 2015a); ii) low temperature  
901 alteration minerals have very low Cl concentrations (section 9.6.2; Table 4); and iii) amphibole  
902 Cl concentrations increase from greenschist- to amphibolite-facies providing evidence for  
903 fluids becoming increasingly saline at depth in the oceanic crust (section 9.6.3).

904           Finally, the concentration range of Cl in pristine mid-ocean ridge glasses is contrasted  
905 with the concentration range in altered oceanic rocks in Fig 19. The pristine glasses include  
906 N-MORB and E-MORB and are variably evolved, with MgO mainly between 4 and 9 wt. %  
907 but including some dacites from the Galapagos Spreading Centre with 1 wt % MgO. The  
908 median Cl concentration of these glasses ( $120 \pm 20$  ppm) is suggested here as a proxy for the  
909 ‘initial’ concentration of Cl in layer 2 (lavas and dykes) of the oceanic crust. In contrast, the  
910 presence of cumulate minerals in layer 3 gabbros implies a much lower initial concentration of  
911 Cl (and other incompatible elements) in deeper portions of the crust. The suggested initial Cl  
912 concentration of layer 2 ( $120 \pm 20$  ppm Cl) is just within uncertainty of the median obtained  
913 for the upper portion of Hole 1256D ( $160^{+140}_{-50}$  ppm Cl; Figs 18 and 19). Considering the high  
914 flux of seawater and very high water/rock ratios in this part of the crust, the lack of pronounced  
915 Cl enrichment demonstrates that the dominant effect of low temperature alteration is probably  
916 halogen remobilisation and exchange of halogens between seawater and the crust, rather than  
917 halogen enrichment. In contrast, the median concentration of Cl in the lower portion of Hole  
918 1256D ( $360^{+120}_{-60}$  ppm Cl) is probably >3-30 times higher than the initial concentration of Cl in

919 the gabbro cumulates (Fig 18). Therefore, it appears that hydrothermal alteration may mobilise  
920 Cl in the upper crust and strongly enrich Cl in the lower crust (Figs 18 and 19). In contrast to  
921 Cl, K exhibits the opposite behaviour, being most enriched during low temperature alteration  
922 in the upper crust. Therefore, the K/Cl ratio, which is commonly used to measure relative Cl  
923 enrichment, changes with increasing crustal depth and alteration much more sharply than the  
924 absolute abundance of either element (Fig 18c).

925

### 926 ***9.6.5 Halogens in serpentinites***

927 The halogen content of seafloor serpentinites has been investigated in several studies (Barnes  
928 et al., 2009; Barnes and Sharp, 2006; Bonifacie et al., 2008; Boschi et al., 2013; Debret et al.,  
929 2014; John et al., 2011; Kendrick et al., 2013b; Kodolányi et al., 2012; Scambelluri et al., 2004;  
930 Sharp and Barnes, 2004). Taken together the data show serpentinites contain from ~100 ppm  
931 to 1 wt. % Cl, with a median concentration of  $1500^{+300}_{-200}$  ppm Cl (Fig 20). The maximum  
932 concentration of Cl in serpentine is somewhat less than amphibole, but serpentinite rocks,  
933 wholly dominated by serpentine, have a higher H<sub>2</sub>O and Cl content than any other major  
934 subduction zone lithology (Scambelluri et al., 1997; Schmidt and Poli, 1998).

935 The I/Cl ratio of serpentinites is not correlated with Cl concentration (Fig 21a);  
936 however, serpentinites have combined Br/Cl and I/Cl that overlap the range of sedimentary  
937 marine pore waters and the serpentinites formed at the greatest distances from mid-ocean ridges  
938 have the highest I/Cl ratios (Fig 22; Kendrick et al., 2013b). These data can be explained if  
939 sedimentary marine pore waters, as well as seawater, are involved in serpentinitisation (Kendrick  
940 et al., 2013b; 2011b). Sedimentary marine pore waters could be particularly important during  
941 serpentinitisation at the slab bend and in the forearc (Fig 5; Ranero et al., 2003). The small  
942 mismatch between serpentinite Br/Cl-I/Cl and sedimentary marine pore waters could be

943 explained in several ways. The high I and Br content of the serpentinites attests to the high  
944 compatibility of all halogens in serpentine. However, it is likely that halogen abundance ratios  
945 are fractionated between serpentinites and serpentinitising fluids. Alternatively, if serpentinites  
946 preserve Br/Cl and I/Cl ratios close to that of the serpentinitising fluids, the data indicate that in  
947 addition to seawater and sediment-derived halogens, some serpentinites contain an additional  
948 small ‘mantle’ component that could be mobilised from igneous lithologies in the overlying  
949 crustal rocks (Figs 22 and 23). Slab fluids with fractionated I/Cl are then required to explain  
950 the highest I/Cl of 0.04 in forearc serpentinites because it is greater than observed in  
951 sedimentary pore waters (Fig 22a; Kendrick et al., 2013b).

952 In contrast to I/Cl and Br/Cl, the F/Cl ratio is negatively correlated with Cl in  
953 serpentinites (Fig 21b) in a similar manner to that observed for amphibole (Fig 17). It is likely  
954 that the compatibility of F is at least as high as the heavy halogens in serpentine, but the  
955 negative relationship between F/Cl and Cl can be explained if serpentinitising fluids introduce  
956 variable quantities of seawater and sediment-derived Cl, Br, and I, and relatively little F (Figs  
957 22 and 23). There are very few combined F/Cl and I/Cl data available for sedimentary pore  
958 waters (Mahn and Gieskes, 2001). However, the low solubility of F in sedimentary pore waters  
959 (Frohlich et al., 1983; Rude and Aller, 1994) suggests F/Cl is likely to be maintained fairly  
960 close to the seawater value. Therefore, the higher F/Cl of serpentinites and some hydrothermal  
961 fluids, relative to seawater, probably results from mobilisation of F from igneous lithologies in  
962 the crust (Fig 23).

963 The median Cl concentration of  $1500_{-200}^{+300}$  ppm in serpentinites corresponds to a  
964 H<sub>2</sub>O/Cl weight ratio of ~80 that is greater than the seawater H<sub>2</sub>O/Cl value of 50. Serpentinites  
965 with much higher Cl concentrations are probably produced as the water ‘drys up’ and the  
966 salinity of the serpentinitising fluid increases (e.g. H<sub>2</sub>O/Cl decreases). Kendrick et al. (2011,  
967 2013b) suggested a water/rock ratio of <0.1 and that the fluid being spent during



968 serpentinisation (e.g. dried up) might be required to explain the preservation of sediment pore  
969 water halogen signatures (Fig 22) and high noble gas concentrations in serpentine. However,  
970 metamorphic salts produced by complete drying up (e.g. Markl and Bucher, 1998) have not  
971 been identified in crushed serpentinites. The nature of the ‘water soluble Cl component’ in  
972 serpentinites is still unclear (Kodolányi et al, 2012) and experimental studies are required to  
973 determine halogen partitioning in serpentinites.

974

### 975 **9.7 Synthesis and future directions**

976 As shown above there are a relatively large number of data available for F, Cl, Br, and  
977 I in sedimentary pore waters and hydrothermal fluids, but the data base for multiple halogens  
978 in minerals within sediments and the crustal basement is much smaller. As a result, while Cl,  
979 Br, and I are known to exhibit systematic behaviour in sedimentary pore waters and the organic  
980 phase within unconsolidated sediment (Figs 2 and 3), the relative abundance ratios of F/Cl,  
981 Br/Cl, and I/Cl and the halogen concentrations in lithified sediments are less well known.  
982 Chlorine and F data, and limited Br and I data, are available for altered basalts and gabbros,  
983 and serpentinites. Despite the limitations imposed by data availability, some general  
984 statements about the most important lithologies and estimates of likely concentration ranges  
985 in key crustal lithologies are possible. This is undertaken below for each of the halogens in a  
986 ‘representative crustal section’ entering a subduction zone. This is undertaken for the crust  
987 immediately prior to subduction, because the final state of the oceanic crust is relevant for  
988 assessing possible fluxes of halogens into the deep mantle and through magmatic arcs, which  
989 is a critical parameter given the role of halogens in complexing metals and facilitating trace  
990 element transport in slab-derived fluids (Migdisov and Williams-Jones, 2014; Yardley, 2005).

991 The representative crustal section investigated comprises 400 m of marine sediment,  
992 1500 m of layer 2 lavas and dykes, 4500 m of layer 3 gabbros, and 500 m of serpentinites (Fig  
993 24). These thicknesses are based on average crust (Chen, 1992; Snow and Edmonds, 2007)  
994 and a band of serpentinite, which could represent either intense local zones of serpentinitisation  
995 primarily formed at slow spreading centres, or 5% serpentinitisation of the uppermost 10 km of  
996 the lithospheric mantle formed at the slab bend (Fig 5). The degree of lithospheric  
997 serpentinitisation is still poorly known, and given that additional serpentinitisation occurs in the  
998 forearc (Bostock et al., 2002), this figure is considered a very conservative lower limit for the  
999 amount of serpentinite subducted into the mantle.

1000 The existing data suggest that Cl concentrations increase with depth in the altered  
1001 oceanic crust (Fig 18). However, for simplicity we assume that the upper 1000 m of the oceanic  
1002 crust, which has been subjected to relatively low temperature alteration, has a median  
1003 concentration of  $160_{-50}^{+140}$  ppm Cl, and that the lower 5000 m has a median concentration of  
1004  $360_{-60}^{+120}$  ppm Cl (cf. Figs 18 and 24). It is possible that away from the subduction zones a  
1005 large portion of the crust, at depths of 4-6 km, could be unaltered. However, it is assumed that  
1006 at the point of subduction, fluids have penetrated the entire crustal section, which is consistent  
1007 with seismic evidence for serpentinitisation of the mantle lithosphere at the slab bend (Fig 5;  
1008 Ranero et al., 2003) and heat flow measurements (Grevemeyer et al., 2005). In this scenario,  
1009 it is likely that at increasing depths, zones of relatively unaltered crust are transected by  
1010 increasingly Cl-rich zones of alteration, reflecting channelized fluid flow within deep fracture  
1011 systems. This would lead to extremely variable concentrations of Cl in the deeper crust, similar  
1012 to that observed in existing drill hole data and dredge samples; for example, Fig 18 shows  
1013 concentrations ranging from 200 to 1200 ppm Cl at ~1200 m in Hole 1256D (Sano et al., 2008).  
1014 In comparison to the oceanic crust, sediments are assumed to have a poorly defined Cl  
1015 concentration of  $700 \pm 500$  ppm (cf. Table 2; Muramatsu and Wedepohl, 1998) and

1016 serpentinites are assigned the median value of  $1500^{+300}_{-200}$  ppm Cl (Figs 20 and 24). These  
1017 figures suggest that the subducting lithosphere could have a bulk Cl concentration on the order  
1018 of 400 ppm (Fig 24). This figure is close to the median value suggested for altered ocean crust  
1019 (Fig 24), and implies that due to its size, the altered ocean crust could be the largest single Cl  
1020 reservoir in subducting slabs (Fig 25). However, it should be stressed that there is considerable  
1021 uncertainty concerning the degree of deep-crust and lithosphere alteration, and that the relative  
1022 sizes of the altered ocean crust and serpentinite reservoirs in Fig 24 could be substantially  
1023 different.

1024 In contrast to Cl, there are fewer data available for F. However, because F is mobilised  
1025 over relatively short distances during alteration and is not significantly introduced by seawater,  
1026 we assume the F concentration in layer 2 of altered ocean crust is similar to that of MORB.  
1027 The average F concentration of MORB is estimated as  $260 \pm 160$  ppm F, based on a F/Nd = 20  
1028  $\pm 12$  (Workman et al., 2006) and Nd of  $\sim 13$  ppm, which is 10 times the primitive mantle value  
1029 (Hofmann, 2003). Serpentinites have typical F concentrations of 10-100 ppm (Debret et al.,  
1030 2014; John et al., 2011), which are enriched compared to depleted mantle values of 11-16 ppm  
1031 F (Pyle and Mather, 2009). We assume this F has been mobilised from overlying lithologies  
1032 in layers 1-3 of the crust (Fig 23). Marine sediments are assigned a concentration of  $1000 \pm$   
1033  $300$  ppm F (Fig 1; Li, 1991; Rude and Aller, 1991). These assumptions suggest that the altered  
1034 oceanic lithosphere contains on the order of  $100 \pm 50$  ppm F (Table 5). Therefore, the altered  
1035 oceanic lithosphere has a F/Cl weight ratio of  $\sim 0.25$  compared to  $\sim 2$  for median MORB, with  
1036 the difference resulting from up to  $\sim 90$  % of crustal Cl being introduced by hydrothermal  
1037 alteration.

1038 The Br and I content of altered oceanic crust is poorly known. It has been suggested  
1039 that low temperature clay-rich alteration could be enriched in I and have higher I/Cl than  
1040 MORB, whereas high temperature amphibole alteration has Br/Cl and I/Cl of less than MORB

1041 (sections 9.6.2 and 9.6.3; Chavrit et al., 2016; Kendrick et al., 2015). If the altered oceanic  
1042 crust retains Br/Cl and I/Cl within a factor of 2 of MORB, we can estimate it has ppb-levels of  
1043 Br and I. In contrast, sediments and serpentinites both have extremely variable Br/Cl and I/Cl  
1044 ratios with ppm levels of Br and I (Tables 2 and 5). In contrast to the altered oceanic crust,  
1045 serpentinites formed in the mantle lithosphere can incorporate substantial Br and I and may  
1046 even preserve the Br/Cl, I/Cl, and F/Cl ratios of the serpentinising fluids (cf. Figs 22 and 23).  
1047 The small amount of data available mean that the average Br/Cl and I/Cl of the serpentinites is  
1048 not known (Fig 22). However, even under the conservative assumptions made above regarding  
1049 the extent of lithospheric serpentinisation (Fig 24), serpentinite rocks rich in chrysotile or  
1050 lizardite have the potential to be a major reservoir of Br and I (Table 5; Fig 25). As a result,  
1051 serpentinites have the potential to be an important pathway for Br and I into subduction zones,  
1052 however, it has been suggested that Br and I are preferentially lost relative to Cl during high  
1053 grade metamorphism and antigoritisation of serpentine meaning that Br and I are unlikely to  
1054 be strongly subducted into the deep mantle (cf. Fig 25; John et al., 2011; Kendrick et al., 2011b,  
1055 2013b, 2014, 2017).

1056 Further work combining the analysis of multiple halogens in hydrothermal fluids is now  
1057 desirable. In particular, analysis of I in hydrothermal fluids together with Br and Cl would help  
1058 confirm if hydrothermal fluids with elevated Br/Cl ratios have interacted with sediments (cf.  
1059 Fig 11). In addition, it is important to improve linkages in understanding between the  
1060 behaviour of halogens in hydrothermal fluids and changes in alteration mineralogy. This is  
1061 required to test the range of conditions under which Br and Cl can be safely regarded as  
1062 behaving conservatively. The possible importance of low temperature alteration for the marine  
1063 I cycle is yet to be evaluated and further data are required for all the halogens in bulk rock  
1064 samples, individual mineral phases, and fluid inclusions within the oceanic crust and  
1065 lithospheric mantle. The extreme heterogeneity of alteration in the oceanic crust and

1066 lithosphere implies a high density of data is required to identify broad trends in changing  
1067 halogen concentration laterally or as a function of depth (e.g. Fig 18).

1068

1069 ***Words = 13,663***

1070

1071 **Acknowledgements.**

1072 Mark A. Kendrick is supported by an Australian Research Council Future Fellowship  
1073 (FT130100141). I am grateful to Zach Sharp and Michael Mottl for their constructive reviews  
1074 of this chapter and also to several colleagues whom I have collaborated with, or discussed  
1075 halogen geochemistry, over the years.

1076

1077 **References**

- 1078 Alt, J., Honnorez, J. (1984) Alteration of the upper oceanic crust, DSDP site 417: mineralogy  
1079 and chemistry. *Contributions to Mineralogy and Petrology* 87: 149-169.
- 1080 Alt, J.C., Mata, P. (2000) On the role of microbes in the alteration of submarine basaltic  
1081 glass: a TEM study. *Earth and Planetary Science Letters* 181: 301-313.
- 1082 Aranovich, L.Ya., Prokofiev, V.Yu., Pertsev, A.N., Bortnikov, N.S., Ageeva, O.A.,  
1083 Bel'tenev, V.E., Borisovsky, S.E., Simakin, S.G. (2015) Composition and origin of a  
1084 K<sub>2</sub>O-rich granite melt in the mid-Atlantic Ridge, 13°34' N: evidence from the  
1085 analysis of melt inclusions and minerals of the gabbro-plagiogranite association.  
1086 *Doklady Earth Sciences* 460: 174–178.
- 1087 Anderson, B.W., Coogan, L.A., Gillis, K.M. (2012) The role of outcrop-to-outcrop fluid flow  
1088 in off-axis oceanic hydrothermal systems under abyssal sedimentation conditions. *J.*  
1089 *Geophys. Res.-Solid Earth* 117: B05 103.
- 1090 Anderson, R.N., Zoback, M.D., Hickman, S.H., Newmark, R.L. (1985) Permeability versus  
1091 depth in the upper oceanic crust - insitu measurements in DSDP Hole 504B, Eastern  
1092 Equatorial Pacific. *Journal of Geophysical Research-Solid Earth and Planets* 90,  
1093 3659-3669. Baker, E.T., 2007. Hydrothermal cooling of midocean ridge axes: Do  
1094 measured and modeled heat fluxes agree? *Earth and Planetary Science Letters* 263:  
1095 140-150.
- 1096 Baker, E.T., German, C.R. (2004) On the global distribution of hydrothermal vent fields, in:  
1097 German, C.R., Lin, J., Parson, L.M. (Eds.), *Mid-Ocean Ridges: Hydrothermal*  
1098 *Interactions between the Lithosphere and Oceans*, pp. 245-266.
- 1099 Barnes, J.D., Cisneros, M. (2012) Mineralogical control on the chlorine isotope composition  
1100 of altered oceanic crust. *Chemical Geology* 326–327: 51-60.
- 1101 Barnes, J.D., Paulick, H., Sharp, Z.D., Bach, W., Beaudoin, G. (2009) Stable isotope (delta  
1102 O-18, delta D, delta Cl-37) evidence for multiple fluid histories in mid-Atlantic  
1103 abyssal peridotites (ODP Leg 209). *Lithos* 110: 83-94.
- 1104 Barnes, J.D., Sharp, Z.D. (2006) A chlorine isotope study of DSDP/ODP serpentinized  
1105 ultramafic rocks: Insights into the serpentinization process. *Chemical Geology* 228:  
1106 246-265.
- 1107 Baturin, G.N., Dubinchuk, V.T. (2011) Mineralogy and chemistry of ferromanganese crusts  
1108 from the Atlantic Ocean. *Geochemistry International* 49: 578-593.

- 1109 Bein, A., Hovorka, S.D., Fisher, R.S., Roedder, E. (1991) Fluid Inclusions in Bedded  
1110 Permian Halite, Palo Duro Basin, Texas - Evidence for Modification of Seawater in  
1111 Evaporite Brine-Pools and Subsequent Early Diagenesis. *Journal of Sedimentary*  
1112 *Petrology* 61: 1-14.
- 1113 Berndt, M.E., Seyfried Jr, W.E., Janecky, D.R. (1989) Plagioclase and epidote buffering of  
1114 cation ratios in mid-ocean ridge hydrothermal fluids: Experimental results in and  
1115 near the supercritical region. *Geochimica et Cosmochimica Acta* 53: 2283-2300.
- 1116 Berndt, M.E., Seyfried, W.E. (1990) Boron, Bromine and Other Trace-Elements as Clues to  
1117 the Fate of Chlorine in Midocean Ridge Vent Fluids. *Geochimica et Cosmochimica*  
1118 *Acta* 54: 2235-2245.
- 1119 Berndt, M.E., Seyfried, W.E. (1997) Calibration of Br/Cl fractionation during subcritical  
1120 phase separation of seawater: Possible halite at 9 to 10 degrees N East Pacific Rise.  
1121 *Geochimica et Cosmochimica Acta* 61: 2849-2854.
- 1122 Bernini, D., Wiedenbeck, M., Dolejs, D., Keppler, H. (2013) Partitioning of halogens  
1123 between mantle minerals and aqueous fluids: implications for the fluid flow regime  
1124 in subduction zones. *Contributions to Mineralogy and Petrology* 165: 117-128.
- 1125 Bideau, D., Hebert, R., Hekinian, R., Cannat, M. (1991) Metamorphism of deep seated rocks  
1126 from the Garrett ultrafast transform (East Pacific Rise near 13-degrees-25'S). *Journal*  
1127 *of Geophysical Research-Solid Earth and Planets* 96: 10079-10099.
- 1128 Bird, P. (2003) An updated digital model of plate boundaries. *Geochem. Geophys. Geosyst.*  
1129 4: 1027.
- 1130 Bischoff, J.L., Dickson, F.W. (1975) Seawater-basalt interaction at 200 degrees C and 500  
1131 bars – Implications for the origin of seafloor heavy-metal deposits and regulation of  
1132 seawater chemistry . *Earth and Planetary Science Letters* 25: 385-397.
- 1133 Bischoff, J.L., Pitzer, K.S. (1989) Liquid-vapor relations for the system NaCl-H<sub>2</sub>O; summary  
1134 of the P-T-x surface from 300 degrees to 500 degrees C. *American Journal of*  
1135 *Science* 289: 217-248.
- 1136 Bischoff, J.L., Rosenbauer, R.J. (1984) The critical point and two-phase boundary of  
1137 seawater, 200–500°C. *Earth and Planetary Science Letters* 68: 172-180.
- 1138 Bischoff, J.L., Rosenbauer, R.J. (1989) Salinity variations in submarine hydrothermal  
1139 systems by layered double diffusive convection. *Journal of Geology* 97: 613-623.
- 1140 Bischoff, J.L., Rosenbauer, R.J., Fournier, R.O. (1996) The generation of HCl in the system  
1141 CaCl<sub>2</sub>-H<sub>2</sub>O: Vapor-liquid relations from 380-500 degrees C. *Geochimica et*  
1142 *Cosmochimica Acta* 60: 7-16.

- 1143 Bobrov, V.A., Phedorin, M.A., Leonova, G.A., Kolmogorov, Y.P. (2005) SR XRF element  
1144 analysis of sea plankton. *Nuclear Instruments & Methods in Physics Research*  
1145 Section a-Accelerators Spectrometers Detectors and Associated Equipment 543:  
1146 259-265.
- 1147 Böhlke, J.K., Irwin, J.J. (1992) Laser microprobe analyses of noble gas isotopes and halogens  
1148 in fluid inclusions: Analyses of microstandards and synthetic inclusions in quartz.  
1149 *Geochim. Cosmochim. Acta* 56: 187-201.
- 1150 Bonifacie, M., Busigny, V., Mevel, C., Philippot, P., Agrinier, P., Jendrzejewski, N.,  
1151 Scambelluri, M., Javoy, M. (2008) Chlorine isotopic composition in seafloor  
1152 serpentinites and high-pressure metaperidotites. Insights into oceanic  
1153 serpentinization and subduction processes. *Geochimica Et Cosmochimica Acta* 72:  
1154 126-139.
- 1155 Bonifacie, M., Jendrzejewski, N., Agrinier, P., Coleman, M., Pineau, F., Javoy, M. (2007)  
1156 Pyrohydrolysis-IRMS determination of silicate chlorine stable isotope compositions.  
1157 Application to oceanic crust and meteorite samples. *Chemical Geology* 242: 187-  
1158 201.
- 1159 Boschi, C., Bonatti, E., Ligi, M., Brunelli, D., Cipriani, A., Dallai, L., D'Orazio, M., Früh-  
1160 Green, G.L., Tonarini, S., Barnes, J.D., Bedini, R.M. (2013) Serpentinization of  
1161 mantle peridotites along an uplifted lithospheric section, Mid Atlantic Ridge at 11°  
1162 N. *Lithos* 178: 3-23.
- 1163 Bostock, M. G., Hyndman, R. D., Rondenay, S., and Peacock, S. M. (2002) An inverted  
1164 continental Moho and serpentinization of the forearc mantle. *Nature* 417: 536-538.
- 1165 Bureau, H., Métrich, N. (2003) An experimental study of bromine behaviour in water-  
1166 saturated silicic melts. *Geochimica et Cosmochimica Acta* 67: 1689-1697.
- 1167 Butterfield, D.A., Jonasson, I.R., Massoth, G.J., Feely, R.A., Roe, K.K., Embley, R.E.,  
1168 Holden, J.F., McDuff, R.E., Lilley, M.D., Delaney, J.R., Pyle, D. (1997) Seafloor  
1169 Eruptions and Evolution of Hydrothermal Fluid Chemistry [and Discussion].  
1170 *Philosophical Transactions: Mathematical, Physical and Engineering Sciences* 355:  
1171 369-386.
- 1172 Campbell, A.C., Bowers, T.S., Measures, C.I., Falkner, K.K., Khadem, M., Edmond, J.M.  
1173 (1988) A time series of vent fluid compositions from 21 degrees N, East Pacific Rise  
1174 (1979, 1981, 1985), and the Guaymas Basin, Gulf of California (1982, 1985).  
1175 *Journal of Geophysical Research-Solid Earth and Planets* 93: 4537-4549.



- 1176 Campbell, A.C., Edmond, J.M. (1989) Halide systematics of submarine hydrothermal vents.  
1177 Nature 342: 168-170.
- 1178 Campbell, A.C., German, C., Palmer, M.R., Gamo, T., Edmond, J.M. (1994) Chapter 11.  
1179 Geochemistry of Hydrothermal Fluids from Escanaba Trough, gorda Ridge,  
1180 Geological, Hydrothermal and Biologic Studies at Escanaba Trough, Gorda Ridge,  
1181 Offshore Northern California USGS Bulletin. USGS, pp. 201-221.
- 1182 Carpenter, R. (1969) Factors controlling the marine geochemistry of fluorine. *Geochimica et*  
1183 *Cosmochimica Acta* 33: 1153-1167.
- 1184 Castelain, T., McCaig, A.M., Cliff, R.A. (2014) Fluid evolution in an Oceanic Core  
1185 Complex: A fluid inclusion study from IODP Hole U1309 D-Atlantis Massif, 30  
1186 degrees N, Mid-Atlantic Ridge. *Geochem. Geophys. Geosyst.* 15: 1193-1214.
- 1187 Chavrit, D., Burgess, R., Sumino, H., Teagle, D. A. H., Droop, G., Shimizu, A., Ballentine,  
1188 C. J. (2016) The contribution of hydrothermally altered ocean crust to the mantle  
1189 halogen and noble gas cycles. *Geochimica et Cosmochimica Acta* 183: 106-124
- 1190 Chen, Y.J. (1992) Oceanic crustal thickness versus spreading rate. *Geophysical Research*  
1191 *Letters* 19: 753-756.
- 1192 Claret, F., Lerouge, C., Laurieux, T., Bizi, M., Conte, T., Ghestem, J.P., Wille, G., Sato, T.,  
1193 Gaucher, E.C., Giffaut, E., Tournassat, C. (2010) Natural iodine in a clay formation:  
1194 Implications for iodine fate in geological disposals. *Geochimica et Cosmochimica*  
1195 *Acta* 74: 16-29.
- 1196 Collins, A.G. (1969) Chemistry of some Andarko Basin brines containing high  
1197 concentrations of iodine. *Chemical Geology* 4: 169-187.
- 1198 Conference Participants (1972) Penrose field conference: Ophiolites. *Geotimes* 17: 24-25.
- 1199 Coogan, L.A., Wilson, R.N., Gillis, K.M., MacLeod, C.J. (2001) Near-solidus evolution of  
1200 oceanic gabbros: insights from amphibole geochemistry. *Geochimica et*  
1201 *Cosmochimica Acta* 65: 4339-4357.
- 1202 Coombs, M. L., Sisson, T. W., and Kimura, J. I. (2004) Ultra-high chlorine in submarine  
1203 Kilauea glasses: evidence for direct assimilation of brine by magma. *Earth and*  
1204 *Planetary Science Letters* 217: 297-313.
- 1205 Cortesogno, L., Gaggero, L., Zanetti, A. (2004) Rare earth and trace elements in amphiboles  
1206 of oceanic gabbros (MARK area, mid-atlantic ridge) at medium to low-temperature  
1207 seafloor alteration. *Ophioliti* 29: 107-123.
- 1208 Cosgrove, M.E. (1970) Iodine in bituminous kimmeridge shales of Dorset Coast, England  
1209 *Geochimica et Cosmochimica Acta* 34: 830-836.

- 1210 Dalou, C.I., Koga, K., Shimizu, N., Boulon, J., Devidal, J.-L. (2012) Experimental  
1211 determination of F and Cl partitioning between lherzolite and basaltic melt.  
1212 Contributions to Mineralogy and Petrology 163: 591-609.
- 1213 Danyushevsky, L.V., Eggins, S.M., Falloon, T.J., Christie, D.M. (2000) H<sub>2</sub>O abundance in  
1214 depleted to moderately enriched mid-ocean ridge magmas; Part I: Incompatible  
1215 behaviour, implications for mantle storage, and origin of regional variations. J.  
1216 Petrol. 41: 1329-1364.
- 1217 Debret, B., Koga, K.T., Nicollet, C., Andreani, M., Schwartz, S. (2014) F, Cl and S input via  
1218 serpentinite in subduction zones: implications for the nature of the fluid released at  
1219 depth. Terra Nova 26: 96-101.
- 1220 deMartin, B.J., Sohn, R.A., Canales, J.P., Humphris, S.E. (2007) Kinematics and geometry of  
1221 active detachment faulting beneath the Trans-Atlantic Geotraverse (TAG)  
1222 hydrothermal field on the Mid-Atlantic Ridge. Geology 35: 711-714.
- 1223 Dick, H.J.B., Lin, J., Schouten, H. (2003) An ultraslow-spreading class of ocean ridge.  
1224 Nature 426: 405-412.
- 1225 Dick, H.J.B., Natland, J.H., Ildefonse, B. (2006) Past and Future Impact of Deep Drilling in  
1226 the Oceanic Crust and Mantle. Oceanography 19: 72-80.
- 1227 Dixon, J.E., Stolper, E.M., Holloway, J.R. (1995) An experimental study of water and carbon  
1228 dioxide solubilities in mid ocean ridge basaltic liquids .1. Calibration and solubility  
1229 models. J. Petrol. 36: 1607-1631.
- 1230 Drever, J.I. (1997) The Geochemistry of Natural Waters: Surface and Groundwater  
1231 Environments, 3rd ed. Prentice-Hall Inc., Upper Saddle River, New Jersey.
- 1232 Driesner, T., Heinrich, C.A. (2007) The system H<sub>2</sub>O-NaCl. Part I: Correlation formulae for  
1233 phase relations in temperature-pressure-composition space from 0 to 1000 °C, 0 to  
1234 5000 bar, and 0 to 1 XNaCl. Geochimica et Cosmochimica Acta 71: 4880-4901.
- 1235 Edmond, J.M., Measures, C., McDuff, R.E., Chan, L.H., Collier, R., Grant, B., Gordon, L.I.,  
1236 Corliss, J.B. (1979) Ridge crest hydrothermal activity and the balances of the major  
1237 and minor elements in the ocean - Galapagos data. Earth and Planetary Science  
1238 Letters 46: 1-18.
- 1239 Elderfield, H., Truesdale, V.W. (1980) On the biophilic nature of iodine in seawater. Earth  
1240 and Planetary Science Letters 50: 105-114.
- 1241 Fehn, U., Lu, Z., Tomaru, H. (2006) <sup>129</sup>I/I ratios and halogen concentrations in pore water of  
1242 Hydrate Ridge and their relevance for the origin of gas hydrates: a progress report,

1243 in: Trehu, A.M., Bohrmann, G., Torres, M.E., Colwell, F.S. (Eds.), Proceedings of  
1244 the Ocean Drilling Program, Scientific Results, pp. 1-25.

1245 Fehn, U., Moran, J.E., Snyder, G.T., Muramatsu, Y. (2007a) The initial  $^{129}\text{I}/\text{I}$  ratio and the  
1246 presence of 'old' iodine in continental margins. Nuclear Instruments and Methods in  
1247 Physics Research Section B: Beam Interactions with Materials and Atoms 259: 496-  
1248 502.

1249 Fehn, U., Snyder, G., Egeberg, P.K. (2000) Dating of pore waters with I-129: Relevance for  
1250 the origin of marine gas hydrates. Science 289: 2332-2335.

1251 Fehn, U., Snyder, G.T., Matsumoto, R., Muramatsu, Y., Tomaru, H. (2003) Iodine dating of  
1252 pore waters associated with gas hydrates in the Nankai area, Japan. Geology 31:  
1253 521-524.

1254 Fehn, U., Snyder, G.T., Muramatsu, Y. (2007b) Iodine as a tracer of organic material:  $^{129}\text{I}$   
1255 results from gas hydrate systems and fore arc fluids. Journal of Geochemical  
1256 Exploration 95: 66-80.

1257 Fisher, A.T. (1998) Permeability within basaltic oceanic crust. Rev. Geophys. 36: 143-182.

1258 Fisher, A.T., Becker, K. (2000) Channelized fluid flow in oceanic crust reconciles heat-flow  
1259 and permeability data. Nature 403: 71-74.

1260 Fisk, M.R., Giovannoni, S.J., Thorseth, I.H. (1998) Alteration of oceanic volcanic glass:  
1261 Textural evidence of microbial activity. Science 281: 978-980.

1262 Floyd, P.A., Fuge, R. (1982) Primary and secondary alkali and halogen element distribution  
1263 in Iceland research drilling project basalts from Eastern Iceland. Journal of  
1264 Geophysical Research 87: 6477-6488.

1265 Fontes, J.C., Matray, J.M. (1993) Geochemistry and origin of formation brines from the Paris  
1266 Basin, France 1. Brines associated with Triassic salts. Chemical Geology 109: 149-  
1267 175.

1268 Fournier, R.O., Thompson, J.M. (1993) Composition of steam in the system NaCl-KCl-H<sub>2</sub>O-  
1269 quartz at 600°C. Geochimica et Cosmochimica Acta 57: 4365-4375.

1270 Foustoukos, D.I., Seyfried, W.E. (2007) Trace element partitioning between vapor, brine and  
1271 halite under extreme phase separation conditions. Geochimica et Cosmochimica  
1272 Acta 71: 2056-2071.

1273 Francois, R. (1987) The influence of humic substances on the geochemistry of iodine in  
1274 nearshore and hemipelagic marine-sediments. Geochimica et Cosmochimica Acta  
1275 51: 2417-2427.

- 1276 Freund, S., Beier, C., Krumm, S., Haase, K.M. (2013) Oxygen isotope evidence for the  
1277 formation of andesitic–dacitic magmas from the fast-spreading Pacific–Antarctic  
1278 Rise by assimilation–fractional crystallisation. *Chemical Geology* 347: 271-283.
- 1279 Frohlich, P.N., Kim, K.H., Jahnke, R., Burnett, W.C., Soutar, A., Deakin, M. (1983) Pore  
1280 water fluoride in Peru continental margin sediments: Uptake from seawater.  
1281 *Geochimica et Cosmochimica Acta* 47: 1605-1612.
- 1282 Fryer, P. (2002) Recent studies of serpentinite occurrences in the oceans: Mantle-ocean  
1283 interactions in the plate tectonic cycle. *Chemie Der Erde-Geochemistry* 62: 257-302.
- 1284 Fuge, R., Johnson, C.C. (1986) The geochemistry of iodine - a review. *Environmental*  
1285 *Geochemistry Health* 8: 31-54.
- 1286 Gall, E.A., Kupper, F.C., Kloareg, B. (2004) A survey of iodine content in *Laminaria*  
1287 *digitata*. *Botanica Marina* 47: 30-37.
- 1288 Gieskes, J.M., Mahn, C. (2007) Halide systematics in interstitial waters of ocean drilling  
1289 sediment cores. *Applied Geochemistry* 22: 515-533.
- 1290 Gieskes, J.M., Mahn, C.L., Schnetzger, B. (2000) Data report: Trace element geochemistry of  
1291 I<sup>-</sup>, Br<sup>-</sup>, F<sup>-</sup>, HPO<sub>4</sub><sup>2-</sup>, Ba<sup>2+</sup>, and Mn<sup>2+</sup> in pore waters of Escanaba Trough, sites 1037 and  
1292 1038, in: Zierenberg, R.A., Fouquet, Y., Miller, D.J., Normark, W.R. (Eds.),  
1293 *Proceedings of the Ocean Drilling Program Scientific Results*. Texas A&M  
1294 University, College Station, TX, pp. 1-16.
- 1295 Gieskes, J.M., Simoneit, B.R.T., Goodfellow, W.D., Baker, P.A., Mahn, C. (2002)  
1296 Hydrothermal geochemistry of sediments and pore waters in Escanaba Trough—  
1297 ODP Leg 169. *Applied Geochemistry* 17: 1435-1456.
- 1298 Gillis, K.M., Meyer, P.S. (2001) Metasomatism of oceanic gabbros by late stage melts and  
1299 hydrothermal fluids: Evidence from the rare earth element composition of  
1300 amphiboles. *Geochem. Geophys. Geosyst.* 2: 2000GC000087.
- 1301 Glasby, G.P. (1973) Mechanisms of enrichment of the rarer elements in marine manganese  
1302 nodules. *Marine Chemistry* 1: 105-125.
- 1303 Glasby, G.P. (1998) The relation between earthquakes, faulting, and submarine hydrothermal  
1304 mineralization. *Marine Georesources & Geotechnology* 16: 145-175.
- 1305 Glasby, G.P., Keays, R.R., Rankin, P.C. (1978) Distribution of rare earth, precious metal and  
1306 other trace elements in recent and fossil deep manganese nodules. *Geochem. J.* 12:  
1307 229-243.

- 1308 Glaus, M.A., Muller, W., Van Loon, L.R. (2008) Diffusion of iodide and iodate through  
1309 Opalinus Clay: Monitoring of the redox state using an anion chromatographic  
1310 technique. *Applied Geochemistry* 23: 3612-3619.
- 1311 Goldberg, W.M., Hopkins, T.L., Holl, S.M., Schaefer, J., Kramer, K.J., Morgan, T.D., Kim,  
1312 K. (1994) Chemical-composition of the sclerotized black coral skeleton  
1313 (coelenterata, Antipatharia) - A comparison of 2 species. *Comparative Biochemistry  
1314 and Physiology B-Biochemistry & Molecular Biology* 107: 633-643.
- 1315 Grevemeyer, I., Kaul, N., Diaz-Naveas, J.L., Villinger, H.W., Ranero, C.R., Reichert, C.  
1316 (2005) Heat flow and bending-related faulting at subduction trenches: Case studies  
1317 offshore of Nicaragua and Central Chile. *Earth and Planetary Science Letters* 236:  
1318 238-248.
- 1319 Hannington, M., Jamieson, J., Monecke, T., Petersen, S., Beaulieu, S. (2011) The abundance  
1320 of seafloor massive sulfide deposits. *Geology* 39: 1155-1158.
- 1321 Hanor, J.S. (1994) Origin of saline fluids in sedimentary basins, in: Parnell, J. (Ed.),  
1322 *Geofluids: Origin, Migration and Evolution of fluids in Sedimentary Basins.*  
1323 *Geological Society Special Publication*, pp. 151-174.
- 1324 Hein, J.R., Koschinsky, A. (2014) 13.11 - Deep-Ocean Ferromanganese Crusts and Nodules,  
1325 in: Turekian, H.D.H.K. (Ed.), *Treatise on Geochemistry (Second Edition)*. Elsevier,  
1326 Oxford, pp. 273-291.
- 1327 Hermann, A.G. (1980) Bromide distribution between halite and NaCl-saturated seawater.  
1328 *Chemical Geology* 28: 171-177.
- 1329 Hess, H.H. (1962) History of Ocean Basins, in: A.E.J., E., James, H.L., Leonard, B.F. (Eds.),  
1330 *Petrologic Studies: A Volume to Honour A.F. Buddington*. Geological Society of  
1331 America, pp. 599-620.
- 1332 Hofmann, A.W. (2003) Sampling Mantle Heterogeneity through Oceanic Basalts: Isotopes  
1333 and Trace Elements, in: Carlson, R.L. (Ed.), *Treatise of Geochemistry Volume 2:  
1334 The Core and Mantle*. Elsevier Ltd., pp. 61-101.
- 1335 Holser, W.T. (1979) Trace elements and isotopes in evaporites, in: Burns, R.G. (Ed.), *Marine  
1336 minerals: Mineralogical Society of America Short Course Notes*, pp. 295-346.
- 1337 Honnorez, J., Kirst, P. (1975) Petrology of rodingites from equatorial mid-Atlantic fracture  
1338 zones and their geotectonic significance. *Contributions to Mineralogy and Petrology*  
1339 49: 233-257.
- 1340 Hovey, J.K., Pitzer, K.S., Tanger, J.C., Bischoff, J.L., Rosenbauer, R.J. (1990) Vapour liquid  
1341 – phase equilibria of potassium chloride water mixtures – Equation-of-state

1342 representation for KCl-H<sub>2</sub>O and NaCl-H<sub>2</sub>O. *Journal of Physical Chemistry* 94: 1175-  
1343 1179.

1344 Huang, Z., Ito, K., Morita, I., Yokota, K., Fukushi, K., Timerbaev, A.R., Watanabe, S.,  
1345 Hirokawa, T. (2005) Sensitive monitoring of iodine species in sea water using  
1346 capillary electrophoresis: vertical profiles of dissolved iodine in the Pacific Ocean.  
1347 *Journal of Environmental Monitoring* 7: 804-808.

1348 Humphris, S.E., Cann, J.R. (2000) Constraints on the energy and chemical balances of the  
1349 modern TAG and ancient Cyprus seafloor sulfide deposits. *J. Geophys. Res.-Solid*  
1350 *Earth* 105: 28477-28488.

1351 Humphris, S.E., Thompson, G. (1978) Hydrothermal alteration of oceanic basalts by  
1352 seawater. *Geochimica et Cosmochimica Acta* 42: 107-125.

1353 Hutnak, M., Fisher, A.T., Harris, R., Stein, C., Wang, K., Spinelli, G., Schindler, M.,  
1354 Villinger, H., Silver, E. (2008) Large heat and fluid fluxes driven through mid-plate  
1355 outcrops on ocean crust. *Nature Geosci* 1: 611-614.

1356 Ichikuni, M. (1979) Uptake of fluoride by aragonite. *Chemical Geology* 27: 207-214.

1357 Ishibashi, J.-i., Sato, M., Sano, Y., Wakita, H., Gamo, T., Shanks Iii, W.C. (2002) Helium  
1358 and carbon gas geochemistry of pore fluids from the sediment-rich hydrothermal  
1359 system in Escanaba Trough. *Applied Geochemistry* 17: 1457-1466.

1360 Ito, E., Anderson, A.T., Jr. (1983) Submarine metamorphism of gabbros from the Mid-  
1361 Cayman Rise: Petrographic and mineralogic constraints on hydrothermal processes  
1362 at slow-spreading ridges. *Contributions to Mineralogy and Petrology* 82: 371-388.

1363 Ito, E., Harris, D.M., Anderson, A.T. (1983) Alteration of Oceanic-Crust and Geologic  
1364 Cycling of Chlorine and Water. *Geochimica et Cosmochimica Acta* 47: 1613-1624.

1365 Ivarsson, M., Lindblom, S., Broman, C., Holm, N.G. (2008) Fossilized microorganisms  
1366 associated with zeolite-carbonate interfaces in sub-seafloor hydrothermal  
1367 environments. *Geobiology* 6: 155-170.

1368 Iwamoto, K., Shiraiwa, Y. (2012) Characterization of Intracellular Iodine Accumulation by  
1369 Iodine-Tolerant Microalgae. *Procedia Environmental Sciences* 15: 34-42.

1370 Jackson, J.C., Ericksen, G.E. (1997) An X-ray diffraction method for semiquantitative  
1371 mineralogical analysis of Chilean nitrate ore. *Revista Geologica De Chile* 24: 45-53.

1372 Jacobson, S. (1975) Dashkesanite: High-Chlorine amphibole from St. Pauls Rocks Equatorial  
1373 Atlantic and Transcaucasia, USSR. *Smithsonian Contributions to Earth Sciences* 14:  
1374 17-22.

- 1375 Jambon, A., Deruelle, B., Dreibus, G., Pineau, F. (1995) Chlorine and bromine abundance in  
1376 MORB: The contrasting behaviour of the Mid-Atlantic Ridge and East Pacific Rise  
1377 and implications for chlorine geodynamic cycle. *Chemical Geology* 126: 101-117.
- 1378 James, R.H., Green, D.R.H., Stock, M.J., Alker, B.J., Banerjee, N.R., Cole, C., German, C.R.,  
1379 Huvenne, V.A.I., Powell, A.M., Connelly, D.P. (2014) Composition of hydrothermal  
1380 fluids and mineralogy of associated chimney material on the East Scotia Ridge back-  
1381 arc spreading centre. *Geochimica et Cosmochimica Acta* 139: 47-71.
- 1382 James, R.H., Rudnicki, M.D., Palmer, M.R. (1999) The alkali element and boron  
1383 geochemistry of the Escanaba Trough sediment-hosted hydrothermal system. *Earth  
1384 and Planetary Science Letters* 171: 157-169.
- 1385 John, T., Scambelluri, M., Frische, M., Barnes, J.D., Bach, W. (2011) Dehydration of  
1386 subducting serpentinite: Implications for halogen mobility in subduction zones and  
1387 the deep halogen cycle. *Earth and Planetary Science Letters* 308: 65-76.
- 1388 Johnson, L., Burgess, R., Turner, G., Milledge, J.H., Harris, J.W. (2000) Noble gas and  
1389 halogen geochemistry of mantle fluids: comparison of African and Canadian  
1390 diamonds. *Geochimica et Cosmochimica Acta* 64: 717-732.
- 1391 Kamenetsky, V.S., Eggins, S.M. (2012) Systematics of metals, metalloids, and volatiles in  
1392 MORB melts: Effects of partial melting, crystal fractionation and degassing (a case  
1393 study of Macquarie Island glasses). *Chemical Geology* 302: 76-86.
- 1394 Kawagucci, S., Chiba, H., Shibash, J.-i., Yamanaka, T., Toki, T., Muramatsu, Y., Ueno, Y.,  
1395 Makabe, A., Inoue, K., Yoshida, N., Nakagawa, S., Nunoura, T., Takai, K.,  
1396 Takahata, N., Sano, Y., Narita, T., Teranishi, G., Obata, H., Gamo, T. (2011)  
1397 Hydrothermal fluid geochemistry at the Iheya North field in the mid-Okinawa  
1398 Trough: Implication for origin of methane in subseafloor fluid circulation systems.  
1399 *Geochem. J.* 45: 109-124.
- 1400 Keevil, N.B. (1942) Vapor pressures of aqueous solutions at high temperatures. *J. Am. Chem.*  
1401 *Soc.* 64: 841-850.
- 1402 Kelley, D.S., Delaney, J.R. (1987) 2-phase separation and fracturing in mid-ocean ridge  
1403 gabbros at temperatures greater than 700-degrees-C. *Earth and Planetary Science  
1404 Letters* 83: 53-66.
- 1405 Kelley, D.S., Fruh-Green, G.L., Karson, J.A., Ludwig, K.A. (2007) The Lost City  
1406 Hydrothermal Field Revisited. *Oceanography* 20: 90-99.

- 1407 Kelley, D.S., Gillis, K.M., Thompson, G. (1993) Fluid evolution in submarine magma-  
1408 hydrothermal systems at the Mid-Atlantic Ridge. *J. Geophys. Res.-Solid Earth* 98:  
1409 19579-19596.
- 1410 Kelley, D.S., Karson, J.A., Blackman, D.K., Fruh-Green, G.L., Butterfield, D.A., Lilley,  
1411 M.D., Olson, E.J., Schrenk, M.O., Roe, K.K., Lebon, G.T., Rivizzigno, P., Party,  
1412 A.T.S. (2001) An off-axis hydrothermal vent field near the Mid-Atlantic Ridge at 30  
1413 degrees N. *Nature* 412: 145-149.
- 1414 Kelley, D.S., Robinson, P.T. (1990) Development of a brine dominated hydrothermal system  
1415 at temperatures of 400-500-degrees-C in the upper level plutonic sequence, Troodos  
1416 Ophiolite, Cyprus. *Geochimica et Cosmochimica Acta* 54: 653-661.
- 1417 Kelley, D.S., Robinson, P.T., Malpas, J.G. (1992) Processes of brine generation and  
1418 circulation in the oceanic crust - Fluid inclusion evidence from the Troodos  
1419 Ophiolite, Cyprus. *J. Geophys. Res.-Solid Earth* 97: 9307-9322.
- 1420 Kendrick, M.A. (2012) High precision Cl, Br and I determination in mineral standards using  
1421 the noble gas method. *Chemical Geology* 292-293: 116-126.
- 1422 Kendrick, M.A., Arculus, R.J., Burnard, P., Honda, M. (2013a) Quantifying brine  
1423 assimilation by submarine magmas: Examples from the Galápagos Spreading Centre  
1424 and Lau Basin. *Geochimica et Cosmochimica Acta* 123: 150-165.
- 1425 Kendrick, M. A., Arculus, R. J., Danyushevsky, L., Kamenetsky, V. S., Woodhead, J., and  
1426 Honda, M. (2014) Subduction-related halogens (Cl, Br and I) and H<sub>2</sub>O in magmatic  
1427 glasses from Southwest Pacific Backarc Basins. *Earth and Planetary Science Letters*  
1428 400: 165-176.
- 1429 Kendrick, M. A., Hemond, C., Kamenetsky, V. S., Danyushevsky, L., Devey, C., Rodemann,  
1430 T., Jackson, M. G., and Perfit, M. R. (2017) Seawater cycled throughout the Earth's  
1431 mantle in partially serpentinised lithosphere. *Nat. Geosci.* in press.
- 1432 Kendrick, M.A., Honda, M., Pettke, T., Scambelluri, M., Phillips, D., Giuliani, A. (2013b)  
1433 Subduction zone fluxes of halogens and noble gases in seafloor and forearc  
1434 serpentinites. *Earth and Planetary Science Letters* 365: 86-96.
- 1435 Kendrick, M.A., Honda, M., Vanko, D.A. (2015b) Halogens and noble gases in  
1436 Mathematician Ridge metagabbros: Implications for oceanic hydrothermal root  
1437 zones and global volatile cycles. *Contributions to Mineralogy and Petrology*, 170: 1-  
1438 20.



- 1439 Kendrick, M.A., Jackson, M.G., Hauri, E., Phillips, D. (2015a) The halogen (F, Cl, Br, I) and  
1440 H<sub>2</sub>O systematics of Samoan lavas: Assimilated seawater, EM2 and high 3He/4He  
1441 components. *Earth and Planetary Science Letters* 410: 197-209.
- 1442 Kendrick, M.A., Kamenetsky, V.S., Phillips, D., Honda, M. (2012a) Halogen (Cl, Br, I)  
1443 systematics of mid-ocean ridge basalts: a Macquarie Island case study. *Geochimica  
1444 et Cosmochimica Acta* 81: 82-93.
- 1445 Kendrick, M.A., Phillips, D., Wallace, M., Miller, J.M. (2011a) Halogens and noble gases in  
1446 sedimentary formation waters and Zn-Pb deposits: A case study from the Lennard  
1447 Shelf, Australia. *Applied Geochemistry* 26: 2089-2100.
- 1448 Kendrick, M.A., Scambelluri, M., Honda, M., Phillips, D. (2011b) High abundances of noble  
1449 gas and chlorine delivered to the mantle by serpentinite subduction. *Nat. Geosci.* 4:  
1450 807-812.
- 1451 Kendrick, M.A., Woodhead, J.D., Kamenetsky, V.S. (2012b) Tracking halogens through the  
1452 subduction cycle. *Geology* 40: 1075-1078.
- 1453 Kennedy, H.A., Elderfield, H. (1987a) Iodine diagenesis in non-pelagic deep sea sediments.  
1454 *Geochimica et Cosmochimica Acta* 51: 2505-2514.
- 1455 Kennedy, H.A., Elderfield, H. (1987b) Iodine diagenesis in pelagic deep sea sediments.  
1456 *Geochimica et Cosmochimica Acta* 51: 2489-2504.
- 1457 Kent, A.J.R., Clague, D.A., Honda, M., Stolper, E.M., Hutcheon, I.D., Norman, M.D.  
1458 (1999a) Widespread assimilation of a seawater-derived component at Loihi  
1459 Seamount, Hawaii. *Geochimica et Cosmochimica Acta* 63: 2749-2761.
- 1460 Kent, A.J.R., Norman, M.D., Hutcheon, I.D., Stolper, E.M. (1999b) Assimilation of  
1461 seawater-derived components in an oceanic volcano: evidence from matrix glasses  
1462 and glass inclusions from Loihi seamount, Hawaii. *Chemical Geology* 156: 299-319.
- 1463 Kent, A.J.R., Peate, D.W., Newman, S., Stolper, E.M., Pearce, J.A. (2002) Chlorine in  
1464 submarine glasses from the Lau Basin: seawater contamination and constraints on  
1465 the composition of slab-derived fluids. *Earth and Planetary Science Letters* 202:  
1466 361-377.
- 1467 Ketsko, V.A., Urusova, M.A., Valyashko, V.M. (1984) Solubility and vapour-pressure of  
1468 solutions in the CaCl<sub>2</sub>-H<sub>2</sub>O system at 250-400-degrees-C. *Zhurnal Neorganicheskoi  
1469 Khimii* 29: 2443-2445.
- 1470 Kigai, I.N., Tagirov, B.R. (2010) Evolution of acidity of hydrothermal fluids related to  
1471 hydrolysis of chlorides. *Petrology* 18: 252-262.

- 1472 Kitano, Y., Okumura, M., Idogaki, M. (1975) Incorporation of sodium, chloride and sulfate  
1473 with calcium carbonate. *Geochem. J.* 9: 75-84.
- 1474 Kleinrock, M.C., Humphris, S.E. (1996) Structural control on seafloor hydrothermal activity  
1475 at the TAG active mound. *Nature* 382: 149-153.
- 1476 Kodolányi, J., Pettke, T., Spandler, C., Kamber, B.S., Gméling, K. (2012) Geochemistry of  
1477 Ocean Floor and Fore-arc Serpentinites: Constraints on the Ultramafic Input to  
1478 Subduction Zones. *J. Petrol.* 53: 235-270.
- 1479 Kruber, C., Thorseth, I.H., Pedersen, R.B. (2008) Seafloor alteration of basaltic glass:  
1480 Textures, geochemistry, and endolithic microorganisms. *Geochem. Geophys.*  
1481 *Geosyst.* 9: Q12002.
- 1482 Kuepper, F.C., Carpenter, L.J., Leblanc, C., Toyama, C., Uchida, Y., Maskrey, B.H.,  
1483 Robinson, J., Verhaeghe, E.F., Malin, G., Luther, G.W., III, Kroneck, P.M.H.,  
1484 Kloareg, B., Meyer-Klaucke, W., Muramatsu, Y., Megson, I.L., Potin, P., Feiters,  
1485 M.C. (2013) In vivo speciation studies and antioxidant properties of bromine in  
1486 *Laminaria digitata* reinforce the significance of iodine accumulation for kelps.  
1487 *Journal of Experimental Botany* 64: 2653-2664.
- 1488 Kullerud, K., Erambert, M. (1999) Cl-scapolite, Cl-amphibole, and plagioclase equilibria in  
1489 ductile shear zones at Nusfjord, Lofoten, Norway: implications for fluid  
1490 compositional evolution during fluid-mineral interaction in the deep crust.  
1491 *Geochimica et Cosmochimica Acta* 63: 3829-3844.
- 1492 Larsen, H.C., Cannat, M., Ceuleneer, G., Fruh-Green, G.L., Kodaira, S., MacLeod, C.,  
1493 Miller, J.M., Seama, N., Tatsumi, Y., Toomey, D. (2009) Oceanic Crustal Structure  
1494 and Formation: IODP and ODP Achievements November 2002 - December 2005,  
1495 in: Szarek, R. (Ed.).
- 1496 le Roux, P.J., le Roex, A.P., Schilling, J.G., Shimizu, N., Perkins, W.W., Pearce, N.J.G.  
1497 (2002) Mantle heterogeneity beneath the southern Mid-Atlantic Ridge: trace element  
1498 evidence for contamination of ambient asthenospheric mantle. *Earth and Planetary*  
1499 *Science Letters* 203: 479-498.
- 1500 le Roux, P.J., Shirey, S.B., Hauri, E.H., Perfit, M.R., Bender, J.F. (2006) The effects of  
1501 variable sources, processes and contaminants on the composition of northern EPR  
1502 MORB (8-10 degrees N and 12-14 degrees N): Evidence from volatiles (H<sub>2</sub>O, CO<sub>2</sub>,  
1503 S) and halogens (F, Cl). *Earth and Planetary Science Letters* 251: 209-231.
- 1504 Leblanc, C., Colin, C., Cosse, A., Delage, L., La Barre, S., Morin, P., Fiévet, B., Voiseux, C.,  
1505 Ambroise, Y., Verhaeghe, E., Amouroux, D., Donard, O., Tessier, E., Potin, P.

1506 (2006) Iodine transfers in the coastal marine environment: the key role of brown  
1507 algae and of their vanadium-dependent haloperoxidases. *Biochimie* 88: 1773-1785.

1508 Lécuyer, C., Dubois, M., Marignac, C., Gruau, G., Fouquet, Y., Ramboz, C. (1999) Phase  
1509 separation and fluid mixing in subseafloor back arc hydrothermal systems: A  
1510 microthermometric and oxygen isotope study of fluid inclusions in the barite-sulfide  
1511 chimneys of the Lau Basin. *Journal of Geophysical Research: Solid Earth* 104:  
1512 17911-17927.

1513 Li, Y.-H., Schoonmaker, J.E. (2003) Chemical composition and mineralogy of marine  
1514 sediments, *Treatise on Geochemistry* pp. 1-35.

1515 Li, Y.H. (1991) Distribution patterns of the elements in the ocean – a synthesis. *Geochimica*  
1516 *et Cosmochimica Acta* 55: 3223-3240.

1517 Liebscher, A., Luders, V., Heinrich, W., Schettler, G. (2006) Br/Cl signature of hydrothermal  
1518 fluids: liquid-vapour fractionation of bromine revisited. *Geofluids* 6: 113-121.

1519 Lu, Z.L., Jenkyns, H.C., Rickaby, R.E.M. (2010) Iodine to calcium ratios in marine carbonate  
1520 as a paleo-redox proxy during oceanic anoxic events. *Geology* 38: 1107-1110.

1521 Lytle, M.L., Kelley, K.A., Hauri, E.H., Gill, J.B., Papia, D., Arculus, R.J. (2012) Tracing  
1522 mantle sources and Samoan influence in the northwestern Lau back-arc basin.  
1523 *Geochemistry, Geophysics, Geosystems* 13: 2012GC004233.

1524 Magenheim, A.J., Spivack, A.J., Michael, P.J., Gieskes, J.M. (1995) Chlorine stable isotope  
1525 composition of the oceanic crust: Implications for Earth's distribution of chlorine.  
1526 *Earth and Planetary Science Letters* 131: 427-432.

1527 Mahn, C.L., Gieskes, J.M. (2001) Halide systematics in comparison with nutrient  
1528 distributions in sites 1033B and 1034B, Saanich Inlet: ODP Leg 169S. *Marine*  
1529 *Geology* 174: 323-339.

1530 Markl, G., Bucher, K. (1998) Composition of fluids in the lower crust inferred from  
1531 metamorphic salt in lower crustal rocks. *Nature* 391: 781-783.

1532 Marks, M. A. W., Kendrick, M. A., Eby, N. G., Zack, T., and Wenzel, T. (2016) The F, Cl,  
1533 Br and I Contents of Reference Glasses BHVO-2G, BIR-1G, BCR-2G, GSD-1G,  
1534 GSE-1G, NIST SRM 610 and NIST SRM 612. *Geostandards and Geoanalytical*  
1535 *Research* 40: 10.1111/ggr.12128

1536 Martin, J.B. (1999) Nonconservative behavior of Br-/Cl- ratios during alteration of  
1537 volcanoclastic sediments. *Geochimica et Cosmochimica Acta* 63: 383-391.

- 1538 Martin, J.B., Gieskes, J.M., Torres, M., Kastner, M. (1993) Bromine and iodine in Peru  
1539 margin sediments and pore fluids: Implications for fluid origins. *Geochimica et*  
1540 *Cosmochimica Acta* 57: 4377-4389.
- 1541 Matthies, D., Troll, G. (1990) Distribution of fluorine in recent marine-sediments related to  
1542 petrographic composition – Bransfield Strait and Northwestern Weddell Sea,  
1543 Antarctica. *Marine Geology* 91: 313-324.
- 1544 McCaffrey, M.A., Lazar, B., Holland, H.D. (1987) The evaporation path of seawater and the  
1545 composition of Br<sup>-</sup> and K<sup>+</sup> with halite. *Journal of Sedimentary Petrology* 57: 928-  
1546 937.
- 1547 McDonough, W.F., Sun, S.-s. (1995) The Composition of the Earth. *Chemical Geology* 120:  
1548 223-253.
- 1549 Melchert, B., Devey, C.W., German, C.R., Lackschewitz, K.S., Seifert, R., Walter, M.,  
1550 Mertens, C., Yoerger, D.R., Baker, E.T., Paulick, H., Nakamura, K. (2008) First  
1551 evidence for high-temperature off-axis venting of deep crustal/mantle heat: The  
1552 Nibelungen hydrothermal field, southern Mid-Atlantic Ridge. *Earth and Planetary*  
1553 *Science Letters* 275: 61-69.
- 1554 Mevel, C. (1988) Metamorphism in Oceanic Layer 3, Goringe Bank, Eastern Atlantic.  
1555 *Contributions to Mineralogy and Petrology* 100: 496-509.
- 1556 Michael, P.J., Cornell, W.C. (1998) Influence of spreading rate and magma supply on  
1557 crystallization and assimilation beneath mid-ocean ridges: Evidence from chlorine  
1558 and major element chemistry of mid-ocean ridge basalts. *J. Geophys. Res.-Solid*  
1559 *Earth* 103: 18325-18356.
- 1560 Michael, P.J., Schilling, J.-G. (1989) Chlorine in mid-ocean ridge magmas: Evidence for  
1561 assimilation of seawater-influenced components. *Geochimica et Cosmochimica Acta*  
1562 53: 3131-3143.
- 1563 Migdisov, A. A. and Williams-Jones, A. E. (2014) Hydrothermal transport and deposition of  
1564 the rare earth elements by fluorine-bearing aqueous liquids. *Mineralium Deposita*  
1565 49: 987-997.
- 1566 Montavon, G., Sabatié-Gogova, A., Ribet, S., Bailly, C., Bessagnet, N., Durce, D., Giffaut,  
1567 E., Landesman, C., Grambow, B. (2014) Retention of iodide by the Callovo-  
1568 Oxfordian formation: An experimental study. *Applied Clay Science* 87: 142-149.
- 1569 Mottl, M.J., Seewald, J.S., Wheat, C.G., Tivey, M.K., Michael, P.J., Proskurowski, G.,  
1570 McCollom, T.M., Reeves, E., Sharkey, J., You, C.F., Chan, L.H., Pichler, T. (2011)

1571 Chemistry of hot springs along the Eastern Lau Spreading Center. *Geochimica et*  
1572 *Cosmochimica Acta* 75: 1013-1038.

1573 Muramatsu, Y., Doi, T., Tomaru, H., Fehn, U., Takeuchi, R., Matsumoto, R. (2007) Halogen  
1574 concentrations in pore waters and sediments of the Nankai Trough, Japan:  
1575 Implications for the origin of gas hydrates. *Applied Geochemistry* 22: 534-556.

1576 Muramatsu, Y., Fehn, U., Yoshida, S. (2001) Recycling of iodine in fore-arc areas: evidence  
1577 from the iodine brines in Chiba, Japan. *Earth and Planetary Science Letters* 192:  
1578 583-593.

1579 Muramatsu, Y., Wedepohl, K.H. (1998) The distribution of iodine in the earth's crust.  
1580 *Chemical Geology* 147: 201-216.

1581 Nakayama, E., Kimoto, T., Isshiki, K., Sohrin, Y., Okazaki, S. (1989) Determination and  
1582 distribution of iodide- and total-iodine in the North Pacific Ocean - by using a new  
1583 automated electrochemical method. *Marine Chemistry* 27: 105-116.

1584 Nehlig, P. (1991) Salinity of oceanic hydrothermal fluids: a fluid inclusion study. *Earth and*  
1585 *Planetary Science Letters* 102: 310-325.

1586 Nehlig, P. (1994) Fracture and permeability analysis in magma-hydrothermal transition zones  
1587 in the Samail Ophiolite (Oman). *J. Geophys. Res.-Solid Earth* 99: 589-601.

1588 Nehlig, P., Juteau, T. (1988) Deep crustal seawater penetration and circulation at ocean ridges  
1589 – Evidence from the Oman ophiolite. *Marine Geology* 84: 209-228.

1590 Ohde, S., Kitano, Y. (1980) Incorporation of fluoride into Ca-Mf carbonate. *Geochem. J.* 14:  
1591 321-324.

1592 Okumura, M., Kitano, Y., Idogaki, M. (1983) Incorporation of fluoride ions into calcite -  
1593 Effect of organic materials and magnesium ions in a parent solution. *Geochem. J.*  
1594 17: 257-263.

1595 Okumura, M., Kitano, Y., Idogaki, M. (1986) Behavior of bromide ions during the formation  
1596 of calcium carbonate. *Marine Chemistry* 19: 109-120.

1597 Oosting, S.E., Von Damm, K.L. (1996) Bromide/chloride fractionation in seafloor  
1598 hydrothermal fluids from 9–10°N East Pacific Rise. *Earth and Planetary Science*  
1599 *Letters* 144: 133-145.

1600 Opdyke, B.N., Walter, L.M., Huston, T.J. (1993) Fluoride content of foraminiferal calcite:  
1601 Relations to life habitat, oxygen isotope composition, and minor element chemistry.  
1602 *Geology* 21: 169-172.

1603 Palme, H., O'Neill, H.S.C. (2003) Cosmochemical estimates of Mantle Composition, in:  
1604 Holland, H., Turekian, K.K. (Eds.), Treatise on Geochemistry. Elsevier, New York,  
1605 pp. 1-38.

1606 Palmer, M.R. (1992) Controls over the chloride concentration of submarine hydrothermal  
1607 vent fluids: evidence from Sr/Ca and  $^{87}\text{Sr}/^{86}\text{Sr}$  ratios. Earth and Planetary Science  
1608 Letters 109: 37-46.

1609 Peacock, S. M. (1990) Fluid Processes in Subduction Zones. Science 248: 329-337.

1610 Pierret, M.C., Clauer, N., Bosch, D., Blanc, G., France-Lanord, C. (2001) Chemical and  
1611 isotopic ( $^{87}\text{Sr}/^{86}\text{Sr}$ ,  $\delta^{18}\text{O}$ ,  $\delta\text{D}$ ) constraints to the formation processes of Red-Sea  
1612 brines. Geochimica et Cosmochimica Acta 65: 1259-1275.

1613 Pinet, P.R. (1992) Oceanography: An Introduction to the Planet Oceanus. West Publishin  
1614 Company, New York.

1615 Price, N.B., Calvert, S.E. (1973) The geochemistry of iodine in oxidised and reduced recent  
1616 marine sediments. Geochimica et Cosmochimica Acta 37: 2149-2158.

1617 Price, N.B., Calvert, S.E. (1977) Contrasting geochemical behaviours of iodine and bromine  
1618 in recent sediments from the Namibian Shelf. Geochimica et Cosmochimica Acta  
1619 41: 1769-1775.

1620 Prichard, H.M., Cann, J.R. (1982) Petrology and mineralogy of dredged gabbro from  
1621 Gettysburg Bank, Eastern Atlantic. Contributions to Mineralogy and Petrology 79:  
1622 46-55.

1623 Proskurowski, G., Lilley, M.D., Seewald, J.S., Fruh-Green, G.L., Olson, E.J., Lupton, J.E.,  
1624 Sylva, S.P., Kelley, D.S. (2008) Abiogenic hydrocarbon production at Lost City  
1625 hydrothermal field. Science 319: 604-607.

1626 Pyle, D.M., Mather, T.A. (2009) Halogens in igneous processes and their fluxes to the  
1627 atmosphere and oceans from volcanic activity: A review. Chemical Geology 263:  
1628 110-121.

1629 Ramos, A.A., Ohde, S., Hossain, M.M.M., Ozaki, H., Sirirattanachai, S., Apurado, J.L.  
1630 (2005) Determination of fluorine in coral skeletons by instrumental neutron  
1631 activation analysis. Journal of Radioanalytical and Nuclear Chemistry 266: 19-29.

1632 Ranero, C.R., Phipps Morgan, J., McIntosh, K., Reichert, C. (2003) Bending-related faulting  
1633 and mantle serpentinization at the Middle America trench. Nature 425: 367-373.

1634 Reed, M.H. (1997) Hydrothermal Alteration and its Relationship to Ore fluid Composition,  
1635 in: Barnes, H.L. (Ed.), Geochemistry of Hydrothermal Ore Deposits. John Wiley &  
1636 Sons, Inc., New York, pp. 303-366.

- 1637 Reeves, E.P., Seewald, J.S., Saccocia, P., Bach, W., Craddock, P.R., Shanks, W.C., Sylva,  
1638 S.P., Walsh, E., Pichler, T., Rosner, M. (2011) Geochemistry of hydrothermal fluids  
1639 from the PACMANUS, Northeast Pual and Vienna Woods hydrothermal fields,  
1640 Manus Basin, Papua New Guinea. *Geochimica et Cosmochimica Acta* 75: 1088-  
1641 1123.
- 1642 Rona, P.A., Denlinger, R.P., Fisk, M.R., Howard, K.J., Taghon, G.L., Klitgord, K.D.,  
1643 McClain, J.S., McMurray, G.R., Wiltshire, J.C. (1990) Major off-axis hydrothermal  
1644 activity on the northern Gorda Ridge. *Geology* 18: 493-496.
- 1645 Rude, P.D., Aller, R.C. (1991) Fluorine mobility during early diagenesis of carbonate  
1646 sediment: An indicator of mineral transformations. *Geochimica et Cosmochimica*  
1647 *Acta* 55: 2491-2509.
- 1648 Rude, P.D., Aller, R.C. (1994) Fluorine uptake by Amazon continental shelf sediment and its  
1649 impact on the global fluorine cycle. *Continental Shelf Research* 14: 883-907.
- 1650 Saal, A.E., Hauri, E.H., Langmuir, C.H., Perfit, M.R. (2002) Vapour undersaturation in  
1651 primitive mid-ocean-ridge basalt and the volatile content of Earth's upper mantle.  
1652 *Nature* 419: 451-455.
- 1653 Sano, T., Miyoshi, M., Ingle, S., Banerjee, N.R., Ishimoto, M., Fukuoka, T. (2008) Boron and  
1654 chlorine contents of upper oceanic crust: Basement samples from IODP Hole  
1655 1256D. *Geochemistry, Geophysics, Geosystems* 9: Q12O15.
- 1656 Scambelluri, M., Müntener, O., Ottolini, L., Pettke, T.T., Vannucci, R. (2004) The fate of B,  
1657 Cl and Li in the subducted oceanic mantle and in the antigorite breakdown fluids.  
1658 *Earth and Planetary Science Letters* 222: 217-234.
- 1659 Scambelluri, M., Piccardo, G.B., Philippot, P., Robbiano, A., Negretti, L. (1997) High  
1660 salinity fluid inclusions formed from recycled seawater in deeply subducted alpine  
1661 serpentinite. *Earth and Planetary Science Letters* 148: 485-499.
- 1662 Schilling, J.G., Bergeron, M.B., Evans, R. (1980) Halogens in the mantle beneath the North  
1663 Atlantic. *Philos. Trans. R. Soc. Lond. Ser. A-Math. Phys. Eng. Sci.* 297: 147-178.
- 1664 Schmidt, M.W., Poli, S. (1998) Experimentally based water budgets for dehydrating slabs  
1665 and consequences for arc magma generation. *Earth and Planetary Science Letters*  
1666 163: 361-379.
- 1667 Seyfried, W.E., Berndt, M.E., Janecky, D.R. (1986) Chloride depletions and enrichments in  
1668 seafloor hydrothermal fluids – constraints from experimental basalt alteration  
1669 studies. *Geochimica et Cosmochimica Acta* 50: 469-475.

1670 Seyfried, W.E., Berndt, M.E., Seewald, J.S. (1988) Hydrothermal alteration processes at mid-  
1671 Ocean Ridges – constraints from diabase alteration experiments, hot spring fluids  
1672 and composition of the oceanic crust. *Canadian Mineralogist* 26: 787-804.

1673 Seyfried, W.E., Bischoff, J.L. (1981) Experimental seawater-basalt interaction at 300-  
1674 degrees-C, 500 bars, chemical-exchange, secondary mineral formation and  
1675 implications for the transport of heavy-metals. *Geochimica et Cosmochimica Acta*  
1676 45: 135-147.

1677 Seyfried, W.E., Ding, K. (1995) The hydrothermal chemistry of fluoride in seawater.  
1678 *Geochimica et Cosmochimica Acta* 59: 1063-1071.

1679 Seyfried, W.E., Jr., Seewald, J.S., Berndt, M.E., Ding, K., Foustoukos, D.I. (2003) Chemistry  
1680 of hydrothermal vent fluids from the Main Endeavour Field, northern Juan de Fuca  
1681 Ridge: Geochemical controls in the aftermath of June 1999 seismic events. *J.*  
1682 *Geophys. Res.* 108: 2429.

1683 Seyfried, W.E., Mottl, M.J. (1982) Hydrothermal alteration of basalt by seawater under  
1684 seawater-dominated conditions. *Geochimica et Cosmochimica Acta* 46: 985-1002.

1685 Shanks, W.C., Bischoff, J.L. (1977) Ore transport and deposition in Red Sea geothermal  
1686 systems – geochemical model. *Geochimica et Cosmochimica Acta* 41: 1507-1519.

1687 Sharp, Z.D., Barnes, J.D. (2004) Water-soluble chlorides in massive seafloor serpentinites: a  
1688 source of chloride in subduction zones. *Earth and Planetary Science Letters* 226:  
1689 243-254.

1690 Sharp, Z. D. and Draper, D. S. (2013) The chlorine abundance of Earth: Implications for a  
1691 habitable planet. *Earth and Planetary Science Letters* 369-370: 71-77.

1692 Siemann, M.G., Schramm, M. (2000) Thermodynamic modelling of the Br partition between  
1693 aqueous solutions and halite. *Geochimica Et Cosmochimica Acta* 64: 1681-1693.

1694 Silantyev S.A., Kostitsyn Yu.A., Cherkashin D.V., Kononkova N.N., Kornienko E.M., Dick  
1695 H.J.B., Kelemen P.B. (2008) Magmatic and metamorphic evolution of the oceanic  
1696 crust in the western flank of the MAR crest zone at 15°44'N: Investigation of cores  
1697 from sites 1275B and 1275D, JOIDES resolution Leg 209. *Petrology* 16, 353-375  
1698 [HYPERLINK "http://elibrary.ru/item.asp?id=13581157"](http://elibrary.ru/item.asp?id=13581157)

1699 Sims, K.W.W., Blichert-Toft, J., Fornari, D.J., Perfit, M.R., Goldstein, S.J., Johnson, P.,  
1700 DePaolo, D.J., Hart, S.R., Murrell, P.J., Michael, P.J., Layne, G.D., Ball, L.A.  
1701 (2003) Aberrant youth: Chemical and isotopic constraints on the origin of off-axis  
1702 lavas from the East Pacific Rise, 9 degrees-10 degrees N. *Geochem. Geophys.*  
1703 *Geosyst.* 4: 2002GC000443.



1704 Sims, K.W.W., Goldstein, S.J., Blichert-toft, J., Perfit, M.R., Kelemen, P., Fornari, D.J.,  
1705 Michael, P., Murrell, M.T., Hart, S.R., DePaolo, D.J., Layne, G., Ball, L., Jull, M.,  
1706 Bender, J. (2002) Chemical and isotopic constraints on the generation and transport  
1707 of magma beneath the East Pacific Rise. *Geochimica et Cosmochimica Acta* 66:  
1708 3481-3504.

1709 Snow, J.E., Edmonds, H.N. (2007) Ultraslow-Spreading Ridges Rapid Paradigm Changes.  
1710 *Oceanography* 20: 90-101.

1711 Spandler, C., Pirard, C. (2013) Element recycling from subducting slabs to arc crust: A  
1712 review. *Lithos* 170: 208-223.

1713 Stakes, D., Moore, W.S. (1991) Evolution of hydrothermal activity on the Juan de Fuca  
1714 Ridge – Observations, mineral ages and Ra isotope ratios. *J. Geophys. Res.-Solid*  
1715 *Earth* 96: 21739-21752.

1716 Staudigel, H., Furnes, H., McLoughlin, N., Banerjee, N.R., Connell, L.B., Templeton, A.  
1717 (2008) 3.5 billion years of glass bioalteration: Volcanic rocks as a basis for  
1718 microbial life? *Earth-Science Reviews* 89: 156-176.

1719 Staudigel, H., Hart, S.R. (1983) Alteration of Basaltic Glass - Mechanisms and Significance  
1720 for the Oceanic-Crust Seawater Budget *Geochimica Et Cosmochimica Acta* 47: 337-  
1721 350.

1722 Staudigel, H., Hart, S.R., Koppers, A.A.P., Constable, C., Workman, R., Kurz, M., Baker,  
1723 E.T. (2004) Hydrothermal venting at Vailulu'u Seamount: The smoking end of the  
1724 Samoan chain. *Geochem. Geophys. Geosyst.* 5: Q02003.

1725 Straub, S.M., Layne, G.D. (2003) The systematics of chlorine, fluorine, and water in Izu arc  
1726 front volcanic rocks: Implications for volatile recycling in subduction zones.  
1727 *Geochimica Et Cosmochimica Acta* 67: 4179-4203.

1728 Stroncik, N., Schmincke, H.U. (2002) Palagonite - a review. *International Journal of Earth*  
1729 *Science* 91: 680-697.

1730 Svensen, H., Jamtveit, B., Yardley, B., Engvik, A. K., Austrheim, H., and Broman, C. (1999)  
1731 Lead and bromine enrichment in eclogite-facies fluids: Extreme fractionation during  
1732 lower-crustal hydration. *Geology* 27: 467-470.

1733 Svensen, H., Banks, D.A., Austrheim, H. (2001) Halogen contents of eclogite facies fluid  
1734 inclusions and minerals: Caledonides, western Norway. *Journal of Metamorphic*  
1735 *Geology* 19: 165-178.

- 1736 Talbi, E.L.H., Honnorez, J., Clauer, N., Gauthier-Lafaye, F., Stille, P. (1999) Petrology,  
1737 isotope geochemistry and chemical budgets of oceanic gabbros-seawater interactions  
1738 in the Equatorial Atlantic. *Contributions to Mineralogy and Petrology* 137: 246-266.
- 1739 Tanaka, K., Ono, T., Fujioka, Y., Ohde, S. (2013) Fluoride in non-symbiotic coral associated  
1740 with seawater carbonate. *Marine Chemistry* 149: 45-50.
- 1741 Tivey, M.A., Schouten, H., Kleinrock, M.C. (2003) A near-bottom magnetic survey of the  
1742 Mid-Atlantic Ridge axis at 26 degrees N: Implications for the tectonic evolution of  
1743 the TAG segment. *J. Geophys. Res.-Solid Earth* 108: B5 2277.
- 1744 Tomaru, H., Fehn, U., Lu, Z.L., Matsumoto, R. (2007a) Halogen systematics in the Mallik  
1745 5L-38 gas hydrate production research well, Northwest Territories, Canada:  
1746 Implications for the origin of gas hydrates under terrestrial permafrost conditions.  
1747 *Applied Geochemistry* 22: 656-675.
- 1748 Tomaru, H., Fehn, U., Lu, Z.L., Takeuchi, R., Inagaki, F., Imachi, H., Kotani, R., Matsumoto,  
1749 R., Aoike, K. (2009) Dating of Dissolved Iodine in Pore Waters from the Gas  
1750 Hydrate Occurrence Offshore Shimokita Peninsula, Japan: 129I Results from the  
1751 D/V Chikyu Shakedown Cruise. *Resource Geology* 59: 359-373.
- 1752 Tomaru, H., Lu, Z., Snyder, G.T., Fehn, U., Hiruta, A., Matsumoto, R. (2007b) Origin and  
1753 age of pore waters in an actively venting gas hydrate field near Sado Island, Japan  
1754 Sea: Interpretation of halogen and 129I distributions. *Chemical Geology* 236: 350-  
1755 366.
- 1756 Tomaru, H., Lu, Z.L., Fehn, U., Muramatsu, Y., Matsumoto, R. (2007c) Age variation of  
1757 pore water iodine in the eastern Nankai Trough, Japan: Evidence for different  
1758 methane sources in a large gas hydrate field. *Geology* 35: 1015-1018.
- 1759 Tribuzio, R., Renna, M.R., Dallai, L., Zanetti, A. (2014) The magmatic-hydrothermal  
1760 transition in the lower oceanic crust: Clues from the Ligurian ophiolites, Italy.  
1761 *Geochimica et Cosmochimica Acta* 130: 188-211.
- 1762 Turekian, K.K., Wedepohl, K.H. (1961) Distribution of the Elements in Some Major Units of  
1763 the Earth's Crust. *Geol. Soc. Am. Bull.* 72: 175-192.
- 1764 Ullman, W.J., Aller, R.C. (1985) The geochemistry of iodine in near-shore carbonate  
1765 sediments. *Geochimica et Cosmochimica Acta* 49: 967-978.
- 1766 Unni, C.K., Schilling, J.G. (1978) Cl and Br Degassing by Volcanism Along Reykjanes  
1767 Ridge and Iceland. *Nature* 272: 19-23.
- 1768 Upstillgoddard, R.C., Elderfield, H. (1988) The role of diagenesis in the Estuarine budgets of  
1769 iodine and bromine. *Continental Shelf Research* 8: 405-430.

- 1770 Vanko, D.A. (1986) High-chlorine amphiboles from oceanic rocks: product of highly-saline  
1771 hydrothermal fluids? *Am. Miner.* 71: 51-59.
- 1772 Vanko, D.A. (1988) Temperature, pressure, and composition of hydrothermal fluids, with  
1773 their bearing on the magnitude of tectonic uplift at mid-ocean ridges, inferred from  
1774 fluid inclusions in oceanic layer 3 rocks. *Journal of Geophysical Research: Solid*  
1775 *Earth* 93: 4595-4611.
- 1776 Vanko, D.A., Bach, W., Roberts, S., Yeats, C.J., Scott, S.D. (2004) Fluid inclusion evidence  
1777 for subsurface phase separation and variable fluid mixing regimes beneath the deep-  
1778 sea PACMANUS hydrothermal field, Manus Basin back arc rift, Papua New  
1779 Guinea. *J. Geophys. Res.-Solid Earth* 109: B03201.
- 1780 Vanko, D.A., Bodnar, R.J., Sterner, S.M. (1988) Synthetic fluid inclusions: VIII. Vapor-  
1781 saturated halite solubility in part of the system NaCl-CaCl<sub>2</sub>-H<sub>2</sub>O, with application to  
1782 fluid inclusions from oceanic hydrothermal systems. *Geochimica et Cosmochimica*  
1783 *Acta* 52: 2451-2456.
- 1784 Vanko, D.A., Bonnin-Mosbah, M., Philippot, P., Roedder, E., Sutton, S.R. (2001) Fluid  
1785 inclusions in quartz from oceanic hydrothermal specimens and the Bingham, Utah  
1786 porphyry-Cu deposit: a study with PIXE and SXRF. *Chemical Geology* 173: 227-  
1787 238.
- 1788 Vanko, D.A., Griffith, J.D., Erickson, C.L. (1992) Calcium-rich brines and other  
1789 hydrothermal fluids in fluid inclusions from plutonic rocks, Oceanographer  
1790 Transform, mid-Atlantic Ridge. *Geochimica et Cosmochimica Acta* 56: 35-47.
- 1791 Von Damm, K.L., Buttermore, L.G., Oosting, S.E., Bray, A.M., Fornari, D.J., Lilley, M.D.,  
1792 Shanks Iii, W.C. (1997) Direct observation of the evolution of a seafloor 'black  
1793 smoker' from vapor to brine. *Earth and Planetary Science Letters* 149: 101-111.
- 1794 Von Damm, K.L., Edmond, J.M., Grant, B., Measures, C.I., Walden, B., Weiss, R.F. (1985)  
1795 Chemistry of submarine hydrothermal solutions at 21 °N, East Pacific Rise.  
1796 *Geochimica et Cosmochimica Acta* 49: 2197-2220.
- 1797 Wanless, V.D., Perfit, M.R., Ridley, W.I., Klein, E. (2010) Dacite Petrogenesis on Mid-  
1798 Ocean Ridges: Evidence for Oceanic Crustal Melting and Assimilation. *J. Petrol.* 51:  
1799 2377-2410.
- 1800 Webster, J.D., Kinzler, R.J., Mathez, E.A. (1999) Chloride and water solubility in basalt and  
1801 andesite melts and implications for magmatic degassing. *Geochimica Et*  
1802 *Cosmochimica Acta* 63: 729-738.

- 1803 Williams, D.L., Von Herzen, R.P., Sclater, J.G., Anderson, R.N. (1974) The Galapagos  
1804 Spreading Centre: Lithospheric Cooling and Hydrothermal Circulation. *Geophysical*  
1805 *Journal International* 38: 587-608.
- 1806 Wong, G.T.F., Brewer, P.G. (1977) Marine chemistry of iodine in anoxic basins. *Geochimica*  
1807 *et Cosmochimica Acta* 41: 151-159.
- 1808 Worden, R.H. (1996) Controls on halogen concentrations in sedimentary formation waters.  
1809 *Mineral. Mag.* 60: 259-274.
- 1810 Workman, R.K., Hauri, E., Hart, S.R., Wang, J., Blusztajn, J. (2006) Volatile and trace  
1811 elements in basaltic glasses from Samoa: Implications for water distribution in the  
1812 mantle. *Earth and Planetary Science Letters* 241: 932-951.
- 1813 Wu, S.-F., You, C.-F., Valsami-Jones, E., Baltatzis, E., Shen, M.-L. (2012) Br/Cl and I/Cl  
1814 systematics in the shallow-water hydrothermal system at Milos Island, Hellenic Arc.  
1815 *Marine Chemistry* 140–141: 33-43.
- 1816 Yang, M., Her, N., Ryu, J., Yoon, Y. (2014) Determination of perchlorate and iodide  
1817 concentrations in edible seaweeds. *International Journal of Environmental Science*  
1818 *and Technology* 11: 565-570.
- 1819 Yardley, B.W.D. (2005) 100th Anniversary Special Paper: Metal concentrations in crustal  
1820 fluids and their relationship to ore formation. *Econ. Geol.* 100: 613-632.
- 1821 You, C.F., Butterfield, D.A., Spivack, A.J., Gieskes, J.M., Gamo, T., Campbell, A.J. (1994)  
1822 Boron and halide systematics in submarine hydrothermal systems: Effects of phase  
1823 separation and sedimentary contributions. *Earth and Planetary Science Letters* 123:  
1824 227-238.
- 1825 Zheng, J., Takata, H., Tagami, K., Aono, T., Fujita, K., Uchida, S. (2012) Rapid  
1826 determination of total iodine in Japanese coastal seawater using SF-ICP-MS.  
1827 *Microchemical Journal* 100: 42-47.
- 1828 Zherebtsova, I.K., Volkova, N.N. (1966) Experimental study of behaviour of trace elements  
1829 in the process of natural solar evaporation of Black Sea water and Lake Sasyk-  
1830 Sivash brine. *Geochemistry international* 3: 656-670.
- 1831 Zierenberg, R.A., Schiffman, P., Jonasson, I.R., Tosdal, R., Pickthorn, W., McClain, J.  
1832 (1995) Alteration of basalt hyaloclastite at the off-axis Sea Cliff hydrothermal field,  
1833 Gorda Ridge. *Chemical Geology* 126: 77-99.
- 1834 Zierenberg, R.A., Shanks Iii, W.C. (1986) Isotopic constraints on the origin of the Atlantis II,  
1835 Suakin and Valdivia brines, Red Sea. *Geochimica et Cosmochimica Acta* 50: 2205-  
1836 2214.

1837

1838

1839

**Table 1. Halogens in seawater and the primitive mantle**

	F ppm	Cl ppm	Br ppb	I ppb
Primitive mantle	25	17-20	50	7-10
Seawater	1.3	19,350	67,300	58
Seawater/PM	0.05	1070	1000-1300	6-7

*Refs: Drever (1997); Elderfield and Truesdale(1980); Huang et al. (2005); preferred primitive mantle concentrations are based on unpublished data*

*McDonough and Sun (1995) and Kamenetsky and Eggins (2012); a selection of recent estimates where summarised by Pyle and Mather (2009)*

**Table 2. Representative concentrations of halogens in marine sediment**

	H <sub>2</sub> O	Cl	F	Br	I
	wt. %	wt. %	ppm	ppm	ppm
<b><i>Fluids and sediments</i></b>					
Seawater	96.5	1.93	1.3	67	0.06
Pore fluids	>95	0.17-2.3	0.5-7	2-260	0.1-220
Unlithified pelagic sediments (including pore fluids)*	30*	1*	1000 ± 300	60 ± 60	30 ± 25
Lithified marine sediments		700 ± 500	1000 ± 300	12 ± 10	4 ± 3
<b><i>Mineral and organic components</i></b>					
Seaweed				<200 ppm	1-500
Seaweed (Kelp)				1,000-2,000	10,000
Plankton			1000 ± 500	1,000-4,000	200-300
Calcite			300 ± 200		<2 ppm*
aragonite			1000 ± 500		
Mg-carbonate			800 ± 500		
Fluorapatite			0.6-2.6		
Clay minerals	5-15	<100 ppm	1000 ± 300		(I adsorbed?)
Mn-crusts/nodules		0.6–1.1	390	28-140	100-900

*References: (Baturin, 1988; Carpenter, 1969; Fehn et al., 2006; Fehn et al., 2000; Fehn et al., 2003; Gieskes and Mahn, 2007; Glasby, 1973; Glasby et al., 1978; Hein and Koschinsky, 2014; John et al., 2011; Kennedy and Elderfield, 1987a, b; Lu et al., 2008; Mahn and Gieskes, 2001; Muinos et al., 2013; Muramatsu et al., 2007; Muramatsu et al., 2001; Muramatsu and Wedepohl, 1998; Ohde and Kitano, 1980; Pyle and Mather, 2009; Rude and Aller, 1991; Tanaka et al., 2013; Tomaru et al., 2007a; Tomaru et al., 2009; Tomaru et al., 2007b; Tomaru et al., 2007c).*

**Table 3. Halogen signatures of fluids in the oceanic lithosphere**

	Salinity	F/Cl	Br/Cl	I/Cl
Seawater	3.5	0.00007	0.0035	0.000003
Sedimentary pore fluids	1-5	0.00005-0.0002	SW*-0.014	SW*-0.04
Vent fluids	0.1-7	0.000006-0.0005	0.001-0.005	SW*-0.001
Crustal brines	10-60	<0.0001	SW*-0.005	SW*-0.00003

*SW\** = seawater

References are given in Table 1 and Figs 3, 11 and 14.



**Table 4. Halogens and water in selected minerals of the Altered Oceanic Lithosphere**

Mineral	H <sub>2</sub> O	Cl	F	Br	I
<b><i>Low to intermediate temperature</i><sup>1</sup></b>					
clay minerals	5-15	21-23	150-400		(adsorbed I ?)
palagonite	40-50	10's ppm		<20 ppm	50 ppb-20 ppm
zeolites	9-20				(adsorbed I ?)
Fe-hydroxides	25-40	>0.4-0.8 wt. % (?)		D <sub>Br/Cl</sub> < 1	
<b><i>High temperature</i><sup>2</sup></b>					
amphibole	2	<100 ppm to ~6 wt. %	<100 ppm to ~7 wt %	<0.5-2 ppm	<5-70 ppb
<b><i>Wide temperature range</i><sup>3</sup></b>					
Carbonate			1000 ± 300 ppm (?)		<2 ppm ?
talc	5-9	400-900 (?)			
serpentine	12-14	100 ppm-1 wt. %	10-100 ppm	1-24 ppm	0.05-45 ppm
fluorapatite	0-1	1000-2000 ppm	1-3 wt. %		
<b><i>Fluid inclusions – contribution to bulk Cl concentration</i></b>					
1 vol. %	0.35	70-200 ppm		250-600 ppb	<1-20 ppb

References:

1 – (Kendrick et al., 2015a; Magenheim et al., 1995; Seyfried et al., 1986; Stroncik and Schmincke, 2002)

2 - (Bideau et al., 1991; Cortesogno et al., 2004; Gillis and Meyer, 2001; Ito and Anderson, 1983; Jacobson, 1975; Nehlig and Juteau, 1988; Prichard and Cann, 1982; Vanko, 1986; Kendrick et al., 2015b).

3 - (Barnes et al., 2009; Bonifacie et al., 2008; Claret et al., 2010; Debret et al., 2014; John et al., 2011; Kendrick et al., 2013b; Sharp and Barnes, 2004).

**Table 5. Summary of halogens in sediments, altered ocean crust, and serpentinites**

	Thickness (km)	F ppm	Cl ppm	Br ppm	I ppm
Marine sediments	0.4	1000 ± 300	700 ± 500	60 ± 60	30 ± 25
Mature/lith. sed		1000 ± 300	700 ± 500	12 ± 10	4 ± 3
AOC – layer 2	1-1.5	260 ± 160	160 <sup>+140</sup> <sub>-50</sub>	0.3 <sup>+0.3</sup> <sub>-0.2</sub>	0.02 <sup>+0.02</sup> <sub>-0.01</sub>
AOC – layer 3	4.5-5	50 ± 40	360 <sup>+120</sup> <sub>-60</sub>	0.7 ± 0.4	0.01 ± 0.01
Serpentinites	0.5	50 ± 40	1500 <sup>+300</sup> <sub>-200</sub>	5 ± 1	1.5 ± 1.5
Bulk lithosphere	6.9	100 ± 50	380 <sup>+140</sup> <sub>-90</sub>	3 ± 2	1.6 ± 1.5

Data from Tables 2 and 4 and Figs 1-23. AOC = Altered Ocean Crust.

1

2 *Fig 1. The F content (ppm) of different types of carbonate. Mg carbonates and aragonite have*  
3 *higher F contents than calcite (Carpenter, 1969; Ohde and Kitano, 1980; Ramos et al., 2005;*  
4 *Rude and Aller, 1991; Tanaka et al., 2013).*

5

6 *Fig 2. Iodine in dry sediments (solid phase) and sedimentary pore waters as a function of depth.*  
7 *a) The top 80 cm of sediments on the Namibian Shelf that contain 2-8 wt % organic carbon*  
8 *are exceptionally enriched in I (Price and Calvert, 1977), but show a typical surface*  
9 *enrichment of I resulting from iodate adsorption (Kennedy and Elderfield, 1987a, b; Price and*  
10 *Calvert, 1977). b) Complex deep sediment profiles on the Nankai Trough show that deeper*  
11 *pore fluids have generally higher I concentrations than shallower pore fluids; this trend is seen*  
12 *most clearly in the top 100 m of the second profile (Muramatsu et al., 2007).*

13

14 *Fig 3. Chlorine, Br and I in sediments and sedimentary pore waters. a) Pore water Br/Cl*  
15 *versus I/Cl on a log-log scale (with linear scale inset). Pore waters define an envelope (shaded*  
16 *grey) extending from seawater (star) and bounded by Br\*/I slopes of 0.6 and 1.3 [Br\* denotes*  
17 *seawater-corrected Br where  $Br^* = Br_{total} - Br_{seawater}$ ;  $Br_{seawater} = 0.0035 \times Cl$  (Kendrick et al.,*  
18 *2011a)]. In contrast to pore waters, the solid phase in Nankai Trough sediments has a higher*  
19 *Br\*/I of  $3 \pm 1$  shown by the yellow envelope. b) I/Cl versus salinity expressed as wt. % NaCl*  
20 *equivalent. Pore fluid chlorinity is close to seawater in most cases, but is significantly altered*  
21 *by the formation and destruction of gas hydrate in some locations. Note that the pore waters*  
22 *have been sampled from IODP drill holes on both passive and convergent continental margins*  
23 *(see Fehn et al., 2000, 2003, 2006; Lu et al., 2008; Mahn and Gieskes, 2001; Muramatsu et*  
24 *al., 2001, 2007; Tomaru et al., 2009; 2007bc).*

25

26 *Fig 4. Schematic diagram showing two end-member styles of oceanic crust. Penrose style*  
27 *homogenous oceanic crust with a well defined layered seismic structure is generated at fast*  
28 *spreading centres (Conference Participants, 1972; Dick et al., 2006). Crustal styles vary at*  
29 *slow spreading centres and may include poorly developed gabbros and dykes or a missing*  
30 *volcanic carapace; peridotites exposed on the seafloor are hydrated to serpentinites and the*  
31 *seismic Moho could represent the hydration front. The diagrams are modified after Dick et al.*  
32 *(2006) with permeability data from Anderson et al. (1985, 2012); Fisher (1998); and Fisher*  
33 *and Becker, (2000). Note that fracture permeability continues to variable and poorly defined*  
34 *depths (see text).*

35

36 *Fig 5. Schematic diagram highlighting the slab bend as an important site for deep (>20 km)*  
37 *fractures and hydrothermal alteration of the lithospheric mantle (see text). Note that fractures*  
38 *at the slab bend provide a possible pathway for sedimentary pore waters to infiltrate the*  
39 *lithosphere.*

40

41 *Fig 6. Comparison of selected elements in seawater and Hanging Garden vent fluids from 21°*  
42 *N on the East Pacific Rise (Von Damm et al., 1985; Li and Schoonmaker, 2003). The diagram*  
43 *shows that relative to the 1:1 line (dashed), most trace elements are strongly enriched in the*  
44 *vent fluids, but that S, F, and P are slightly depleted and Mg is quantitatively removed from*  
45 *the vent fluids. Note that the Hanging Garden Vent fluids have near seawater salinity and that*  
46 *this diagram uses a log scale meaning that small variations in concentration (e.g. a factor of*  
47 *2) cannot be easily evaluated (see Fig 7).*

48

49 *Fig 7. Ca/Na versus K/Na weight ratios of vent fluids for which Cl and Br data are available*  
50 *(below). Vent fluids are variably enriched in K and Ca, relative to Na in seawater; the*  
51 *seawater ratios are shown by the star (Butterfield et al., 1990; Ishibashi et al., 1994; James*  
52 *et al., 1995; James et al., 2014; Mottl et al., 2011; Pester et al., 2012; Reeves et al., 2011;*  
53 *Seyfried et al., 2011; Seyfried et al., 2003; Von Damm, 2000; Von Damm et al., 1998; Von*  
54 *Damm et al., 1997; Von Damm et al., 2003).*

55

56 *Fig 8. Temperature and salinity data for selected vent fluids. Note that the data show*  
57 *maximum vent temperature and that most of the salinities are for end-member fluids with zero*  
58 *Mg. A conjugate brine and vapour pair emitted from vent F at 9° N on the East Pacific Rise is*  
59 *indicated (below; Von Damm et al., 1997). The data are from numerous sources (Butterfield*  
60 *et al., 1990; Edmond et al., 1979; Ishibashi et al., 1994; James et al., 1995; 2014; Kawagucci*  
61 *et al., 2011; Mottl et al., 2011; Pester et al., 2012; Reeves et al., 2011; Seyfried et al., 2003,*  
62 *2011; Von Damm et al., 1997, 1998, 2000, 2003, 2005; Wu et al., 2012).*

63

64 *Fig 9. Phase diagrams for the binary H<sub>2</sub>O-NaCl system. a) pressure versus temperature and*  
65 *b) pressure versus wt. % NaCl. Note that the approximate depth of different crustal units under*  
66 *hydrostatic pressure is shown and that the wt. % NaCl scale switches from log to linear at 10*  
67 *wt. %. Part a shows the critical curve, L-V-S boundary that separates the vapour-salt field and*  
68 *the critical point of seawater estimated from 3.2 wt.% NaCl solution. Part b shows the critical*  
69 *curve, liquid-salt field, and isotherms that define the two phase field at selected temperatures.*  
70 *The effects of depressurisation are shown for 4 points (see text). Data and equations used to*  
71 *construct the figures are from Bischoff and Pitzer (1989) and Driesner and Heinrich (2007).*

72

73 *Fig 10. Phase diagrams for various binary salt systems. a) pressure versus temperature plot*  
74 *showing the critical curves for H<sub>2</sub>O-NaCl and H<sub>2</sub>O-CaCl<sub>2</sub>, and the L-V-S curves for the H<sub>2</sub>O-*  
75 *NaCl, K/Cl, and CaCl<sub>2</sub> systems. Note that the vapour-salt field shrinks back from a maximum*  
76 *size in the H<sub>2</sub>O-NaCl system to a minimum size in the H<sub>2</sub>O-CaCl<sub>2</sub> system. b) pressure versus*  
77 *molar equivalent CaCl<sub>2</sub>, HCl, and Ca(OH)<sub>2</sub>. The binary H<sub>2</sub>O-CaCl<sub>2</sub> system differs to the H<sub>2</sub>O-*  
78 *NaCl system in that hydrolysis occurs under high temperature - low pressure conditions (see*

79 *text). Data and equations used to construct the figures are from Bischoff and Pitzer (1989);*  
80 *Bischoff et al.(1996); Driesner and Heinrich (2007); Hovey et al. (1990) and Ketsko et al.*  
81 *(1984).*

82

83 *Fig 11. The halogen systematics of hydrothermal vent fluids: a) F/Cl versus Br/Cl; b) Br/Cl*  
84 *versus salinity; and c) I/Cl versus Br/Cl (Butterfield et al., 1990; Campbell and Edmond, 1989;*  
85 *Campbell et al., 1994; Edmond et al., 1979; Gieskes et al., 2000; 2002; Ishibashi et al., 2002;*  
86 *James et al., 1999, 2014; Kawagucci et al., 2011; Mottl et al., 2011; Oosting and Von Damm,*  
87 *1996; Reeves et al., 2011; Schmidt et al., 2007, 2011; Seyfried et al., 2003; Von Damm, 1985,*  
88 *1997, 1998, 2000, 2003, 2005; Wu et al., 2012; You et al., 1994).*

89

90 *Fig 12. Halogens in pristine glasses and their weakly altered or palagonitised counterparts*  
91 *from Macquarie Island and Samoa (Kendrick et al., 2012, 2015a).*

92

93 *Fig 13. Photomicrographs of vapour and brine fluid inclusions in a quartz vein hosted by*  
94 *amphibolite metagabbro from layer 3 of the crust. This sample (7-45), dredged from the*  
95 *Mathematician Ridge of the Pacific Ocean, has been described in detail by Vanko (1988) and*  
96 *Kendrick et al. (2015b). The vapour bubbles have a high degree of fill in the vapour inclusions.*  
97 *In contrast, brine inclusions have much smaller vapour bubbles and visible halite daughter*  
98 *minerals which have a bright green hue and cubic form.*

99

100 *Fig 14. Schematic diagram illustrating the double diffusive convection concept of Bischoff and*  
101 *Rosenbauer (1989). This model predicts brines are segregated from vapours and preferentially*  
102 *retained in deeper portions of the crust. The presence of brines may help explain some styles*  
103 *of alteration and Cl-rich amphiboles. The ultimate fate of the brines may be to be diluted by*  
104 *lower salinity fluids and flushed out of the crust, to migrate laterally and leak from ridge flanks*  
105 *or be assimilated by magmas (Fig 16).*

106

107 *Fig 15. Halogens in fluid inclusions and amphibole separated from Mathematician Ridge*  
108 *amphibolites and metagabbros. Fluid inclusions were analysed by crushing vein minerals*  
109 *(quartz and epidote) and the amphibole wall-rock in vacuum (Kendrick et al., 2015b). Note*  
110 *that the range of fluid inclusion compositions is very similar to the composition of brines*  
111 *assimilated by submarine magmas dredged from the Lau Basin, Galapagos Spreading Centre*  
112 *and Samoa (Fig 16; Kendrick et al., 2013a; 2015a).*

113

114 *Fig 16. Halogens in magmatic glasses affected by brine assimilation. a) K/Cl versus H<sub>2</sub>O/Cl;*  
115 *b) F/Cl versus H<sub>2</sub>O/Cl; c) Br/Cl versus K/Cl; and d) Br/Cl versus I/Cl (Kendrick et al., 2013a;*

116 2015a; le Roux et al., 2006; Lytle et al., 2012; Wanless et al., 2011). The mantle field is defined  
117 by Kendrick et al., (2012, 2013a; 2014, 2015a). Brines have K/Cl and F/Cl of <0.1 (e.g. Figs.  
118 8) and H<sub>2</sub>O/Cl that is proportional to salinity (parts a and b). The altered ocean crust (AOC)  
119 is assumed to have low K/Cl and high H<sub>2</sub>O/Cl based on existing data and the relatively low  
120 compatibility of Cl in hydrous minerals compared to H<sub>2</sub>O (Ito et al., 1983; Sano et al., 2008).

121

122

123 Fig 17. F/Cl versus Cl concentration for amphiboles in the oceanic crust. The data of Coogan  
124 and Cullen (2009) and Cortesogno et al. (2004) were obtained by ion microprobe, whereas the  
125 data of Gillis and Meyer (2001) and Vanko (1986) are based on electron microprobe analyses.

126

127 Fig 18. The concentrations of a) Cl and b) K and c) the K/Cl ratio of whole rock samples from  
128 IODP Hole 1256D in the East Pacific is shown as a function of depth below the seafloor. The  
129 data are from Sano et al. (2008) and Barnes and Cisneros (2012) (green dots in part a). The  
130 alteration mineralogy shown on the figure is simplified. The median Cl and K concentrations  
131 of low and high temperature alteration zones, with 2σ uncertainties, are shown for comparison.

132

133 Fig 19. The Cl concentrations of pristine MORB glasses and altered ocean crust. The data  
134 define log-normal distributions that are typical of trace elements. The AOC is indicated to have  
135 twice the Cl content of pristine crust on average. Glass data include N-MORB, E-MORB, and  
136 evolved glasses from the Galapagos spreading centre that have assimilated seawater Cl  
137 (Danyushevsky et al., 2000; Kamenetsky and Eggins, 2012; Kendrick et al., 2012a, 2013a; Le  
138 Roux et al., 2002; Michael and Cornell, 1998; Saal et al., 2003; Sims et al., 2002; 2003).  
139 Altered Ocean Crust data are from Barnes and Cisneros (2012), Bonifacie et al. (2007), Floyd  
140 and Fuge (1982), Magenheim et al. (1995), and Sano et al. (2008).

141

142 Fig 20. Histogram and probability density function of serpentinite Cl concentration data. As  
143 with all trace elements, Cl tends toward a log-normal distribution, meaning the median is  
144 better defined than the mean. Data from Barnes et al (2006, 2009), Bonifacie et al. (2008),  
145 Debret et al. (2014), John et al. (2011), Kendrick et al. (2013b), Kodolanyi et al (2012),  
146 Scambelluri et al. (2004) and Sharp and Barnes (2004).

147

148 Fig 21. Halogen abundance ratios as a function of Cl concentration (ppm) in lizardite and  
149 chrysotile 'pre-subduction' serpentinites. a) I/Cl and b) F/Cl (antigorite serpentinites are not  
150 included in these plots). The data of Kendrick et al. (2013b) are differentiated the same way as  
151 in Figure 22. Additional data are from John et al. (2011) and Debret et al. (2014).

152

153 *Fig 22. Br/Cl versus I/Cl for serpentinites: a) linear scale and b) log-log scale. The trend of*  
154 *sedimentary marine pore waters (Fig. 3), gas hydrate, MORB, and the compositions on*  
155 *amphibole and mica are shown for reference. Serpentinite data from Kendrick et al. (2011b,*  
156 *2013b); MORB field from Kendrick et al. (2013a); mica/amphibole data from Kendrick (2012)*  
157 *and Kendrick et al. (2015b), see Fig 15.*

158

159 *Fig 23. Serpentinite F/Cl versus I/Cl data. Serpentinite data from John et al. (2011). Pore*  
160 *fluid data from Gieskes and Mahn (2007). Escanaba Trough high  $^3\text{He}/^4\text{He}$  pore fluid data*  
161 *(representative of hydrothermal fluids) from Gieskes et al. (2002).*

162

163 *Fig 24. Schematic diagram of a representative, oceanic lithospheric cross section with*  
164 *estimated Cl concentrations at the point of subduction. Note that the average extent of*  
165 *alteration in the deep crust and lithospheric mantle are poorly defined and these figures*  
166 *assume significant alteration at the slab bend prior to subduction (see text for discussion).*

167

168 *Fig 25. Pie charts showing the relative importance of sediments, altered ocean crust and*  
169 *serpentinites as reservoirs for F, Cl, Br and I in the oceanic lithosphere, under the assumptions*  
170 *used to construct Fig 24 (Table 5; section 9.7).*

171